

# Statistical Inference in Causal Partial Identification with Smooth Densities

Sirui Lin<sup>1</sup>, Zijun Gao<sup>\*2</sup>, José Blanchet<sup>1</sup>, and Peter Glynn<sup>†1</sup>

<sup>1</sup>Department of Management Science and Engineering, Stanford University

<sup>2</sup>Marshall School of Business, University of Southern California

February 25, 2026

## Abstract

Many causal quantities are only partially identifiable due to the inherent missingness of potential outcomes, and the associated partial identification (PI) sets can be obtained by solving an optimal transport (OT) problem. Covariates often provide additional information about the potential outcomes and thus yield tighter PI sets, which can be obtained via conditional optimal transport (COT). However, COT-based PI set estimators are susceptible to the curse of dimensionality in the covariates and outcomes, which precludes the asymptotic normality and hinders statistical inference. In this paper, we exploit smoothness in the marginal densities of covariates and potential outcomes and develop a wavelet-based primal method for COT with multivariate outcomes and covariates. Moreover, for quadratic cost functions, we establish a stability result for COT and prove asymptotic normality of the proposed estimator. This characterization of the asymptotic distribution enables valid statistical inference for the partial identification set. Empirically, we validate the estimation and inference performance of our approach through numerical experiments in comparison with existing benchmarks.

**Keywords:** Causal inference; partial identification; conditional optimal transport; curse of dimensionality; smooth density estimation; wavelet methods.

## 1 Introduction

We study statistical inference for causal estimands that are only partially identifiable under the potential outcome framework. The target is a partial identification (PI) set, which can be characterized through an optimal transport (OT) formulation [14]. When covariates are available, conditional optimal transport (COT) yields tighter PI sets by conditioning on the covariate distribution, thus provides a natural framework for inference in modern observational and experimental datasets [25, 30, 10].

The problem is important for causal inference because PI sets quantify uncertainty caused by missing counterfactual outcomes, and their widths directly inform decisions in policy evaluation, fairness assessments, and treatment effect analysis. In particular, PI sets can be interpreted as sharp bounds on counterfactual distributions or causal estimands, which makes them central to counterfactual inference. At the same time, COT is of independent interest in OT theory as a conditional analogue of Wasserstein distances, closely related to adapted Wasserstein metrics studied in stochastic and dynamic settings [3]. Thus, advances in COT estimation and inference have immediate implications for both causal inference and statistical OT.

This perspective connects causal inference with statistical OT, an area with rapidly developing theory and methods [44, 38, 37, 22, 32, 21]. This momentum reflects OT’s broad impact across econometrics [13], image analysis and signal processing [41, 4, 27], generative modeling [2, 16, 18, 45], distributional robustness [35,

\*The first two authors contributed equally to this work.

†Emails: zijungao@marshall.usc.edu, siruilin, jose.blanchet, glynn@stanford.edu

28, 5], and finance/model risk [47, 36, 3]. Against this broader backdrop, we focus on statistical inference for causal PI sets via conditional optimal transport.

Current approaches to COT-based PI sets face substantial limitations. Dual formulations can yield valid confidence sets but may be conservative and require strong, hard-to-verify assumptions on potential functions [25, 24]. Penalization and discretization approaches reduce COT to OT at the cost of conservative or slow convergence rates and an acute curse of dimensionality in the covariates and outcomes [33, 29, 30]. Quantile regression can provide asymptotically exact confidence sets but is limited to scalar outcomes [9]. Sampling-based methods learn transport maps or samplers rather than the optimal objective value that defines the PI set [20]. Overall, existing methods do not provide asymptotically normal estimators with practical inference for multivariate outcomes in high-dimensional covariate settings.

We address these challenges with a smoothness-based, primal COT estimator built on wavelet expansions of the observable marginal densities, inspired by recent advances in statistical OT [22, 37, 32]. Unlike dual approaches that require smoothness or regularity of Kantorovich potentials and involve solving optimization problems over function spaces to recover the dual potentials [25, 24], our primal estimator instead exploits smoothness of the densities, an assumption that is more directly verifiable in practice since the densities are observable but potentials are not. The resulting estimator simply plugs in a smooth density estimate to compute the COT value, without the need to solve any optimization problem. Under smoothness assumptions, we establish faster convergence rates for general Lipschitz costs, and for quadratic costs we prove a COT stability result that leads to asymptotic normality and valid confidence sets.

Our contributions span both causal PI inference and COT theory. On the causal side, we provide a principled inferential procedure with improved rates and asymptotically normal confidence sets; to our knowledge, this is the first PI inference approach via COT that delivers asymptotic normality for multivariate outcomes under smoothness. On the OT side, we establish a stability-based central limit theorem for conditional transport under quadratic costs, extending smooth OT results to the conditional setting; to our knowledge, this is the first such CLT for conditional optimal transport, as existing OT CLTs do not cover conditional transport values. A direct comparison of convergence rates and assumptions with prior COT estimators appears in Table 1. The following points summarize the methodological, theoretical, and empirical contributions.

1. We develop a primal, smoothness-based estimator for COT using wavelet expansions of observable marginal densities, complementing dual approaches that rely on potential smoothness [25, 24]. Under smoothness conditions, we establish convergence rates for general Lipschitz costs, demonstrating fast estimation accuracy for causal PI sets.
2. For quadratic costs, we generalize OT stability to the COT setting and leverage it to prove asymptotic normality and conduct valid statistical inference for causal PI sets.
3. We provide empirical evidence that the proposed estimator improves the estimation accuracy over existing COT benchmarks and asymptotically controls the type I error for inference.

**Organization.** Section 2 introduces the potential outcomes framework, conditional optimal transport, and wavelet estimation. Section 3 presents the wavelet-based COT estimator and its convergence rates. Section 3.3 focuses on quadratic costs and develops the COT stability result and asymptotic normality. Section 4 reports experimental results. Section 5 concludes with limitations and future directions. All proofs and additional empirical results appear in the supplementary materials.

**Notation.** We denote  $[n] = \{1, \dots, n\}$ ,  $n \wedge m = \min(n, m)$ ,  $n \vee m = \max(n, m)$ . We denote by  $\mathcal{P}(\Omega)$  the set of probability measures on  $\Omega$ . We use  $\mathcal{P}_{\text{ac}}(\Omega)$ , for  $\Omega \subseteq \mathbb{R}^d$ , to denote the set of probability measures that are absolutely continuous with respect to the Lebesgue measure on  $\mathbb{R}^d$ . We use  $\mu_{Y,Z}$  to denote the probability distribution (and its associated measure on  $\mathcal{Y} \times \mathcal{Z}$ ) of  $(Y, Z)$  under  $\mu$ , with  $\mu_Z$  denoting the marginal distribution of  $Z$ , and  $\mu_Y^z$  the conditional distribution of  $Y$  given  $Z = z$ . By  $\mu = \mu_Z \otimes \mu_Y^z$ , we mean that for any measurable function  $g$ ,  $\int g d\mu = \int_{\mathcal{Z}} \int_{\mathcal{Y}} g(z, y) d\mu_Y^z(y) d\mu_Z(z)$ . We denote the set of the joint couplings  $\pi$  with marginals  $\mu, \nu \in \mathcal{P}(\mathcal{X})$  ( $\mathcal{X}$  may be  $\mathcal{Y}$ ,  $\mathcal{Z}$  or  $\mathcal{Y} \times \mathcal{Z}$ ) by

$$\Pi(\mu, \nu) \triangleq \{\pi \in \mathcal{P}(\mathcal{X}^2) : \pi_X = \mu, \pi_{X'} = \nu\}. \quad (1)$$

Given a density function  $f(y, z)$ , we denote its marginal density of  $z$  by  $f_Z(z)$ , and the conditional density of  $y$  given  $z$  by  $f(y | z) = f(y, z)/f_Z(z)$ . Given a measurable objective function  $h$  and probability distributions  $P, Q \in \mathcal{P}(\mathbb{R}^{d_x})$ , the optimal transport distance is defined as

$$W_h(P, Q) \triangleq \min_{\pi \in \Pi(P, Q)} \mathbb{E}_\pi[h(X, X')],$$

When  $h(x, x') = \|x - x'\|_2^p$ , we denote  $W_p(P, Q) = W_h(P, Q)^{\frac{1}{p}}$ , which is the so-called Wasserstein  $p$ -distance.

For joint distributions  $P$  and  $Q$  on  $\mathcal{Y} \times \mathcal{Z}$ , we write  $\phi_Z$  and  $\psi_Z$  for the Kantorovich potentials associated with the conditional laws  $P_Y^z$  and  $Q_Y^z$ . We use  $P_Z$  to denote the marginal distribution of  $Z$  induced from  $P$ , and similarly for  $Q_Z$ . We use  $W_p(P, Q)$  for the Wasserstein- $p$  distance between  $P$  and  $Q$ , and  $CW_p(P, Q)$  for the conditional Wasserstein- $p$  distance defined as  $(\mathbb{E}[W_p(P(Y | Z), Q(Y | Z))^p])^{1/p}$ .

## 2 Preliminary

### 2.1 Potential Outcome Model and Conditional Optimal Transport

Suppose there are  $2n$  units, and each unit is associated with two potential outcomes  $Y_i(0)$  and  $Y_i(1) \in [0, 1]^{d_Y}$  (see, e.g., [40]). Specifically,  $Y_i(0), Y_i(1)$  is the outcome under control, treatment, respectively. We allow  $d_Y \geq 1$ , so that the outcome, normalized to  $[0, 1]^{d_Y}$ , may be vector-valued. This setting naturally arises in applications such as clinical trials with primary and secondary outcomes, physics experiments where outcomes correspond to two- or three-dimensional spatial locations, and policy evaluations involving multiple aspects, such as effectiveness and cost. In addition, we suppose each unit also comes with a covariate vector  $Z_i \in [0, 1]^{d_Z}$ ,  $d_Z \geq 1$ . We consider the following super-population model [23] for  $(Y_i(0), Y_i(1), Z_i)$ ,

$$(Y_i(0), Y_i(1), Z_i) \stackrel{\text{i.i.d.}}{\sim} \mu, \quad (2)$$

where  $\mu$  denotes an unknown joint distribution. This super-population model satisfies the standard stable unit treatment value assumption (SUTVA) [23], as described in the first paragraph of Section 2.1.

Each unit receives a binary treatment assignment  $W_i \in \{0, 1\}$ , where  $W_i = 1$  indicates treatment and  $W_i = 0$  indicates control, and only the potential outcome corresponding to the received treatment level is observed, i.e.,  $Y_i = Y_i(W_i)$ . For the treatment assignment, we focus on a completely randomized design with half of the units assigned to the treatment, that is,

$$(W_i)_{i=1}^{2n} \sim \text{Uni}\left\{w \in \{0, 1\}^{2n} : \sum_{i=1}^{2n} w_i = n\right\}. \quad (3)$$

Our approach and analysis can be generalized to assignment mechanisms satisfying the unconfoundedness and the overlap assumptions in [23]. Under conditions (2) and (3), the outcome-covariate distributions of  $(Y_i(1), Z_i)$  and  $(Y_i(0), Z_i)$  are identifiable from the observed data. We use  $P$  to denote the distribution of  $(Y_i(0), Z)$  and  $Q$  to denote the distribution of  $(Y_i(1), Z)$ , and write  $p$  and  $q$  for their densities when they exist. At the sample level, we introduce the notation  $(Y_i(w), Z_i(w)) := (Y_i(w), Z_i)$  if  $W_i = w$  for  $w = 0, 1$ . Reindexing the sample, we will denote the sample from treatment group as  $\mathcal{S}_1 := ((Y_i(1), Z_i(1)), i = 1, \dots, n)$  and sample from control group as  $\mathcal{S}_0 := ((Y_i(0), Z_i(0)), i = 1, \dots, n)$ , such that  $\mathcal{S}_1$  can be viewed as an i.i.d. sample from  $Q$  and  $\mathcal{S}_0$  can be viewed as an i.i.d. sample from  $P$ , both with size  $n$ .

In this paper, we focus on causal estimands of the form

$$V \triangleq \mathbb{E}_\mu[h(Y(0), Y(1))]. \quad (4)$$

Here,  $h : \mathcal{Y} \times \mathcal{Y} \rightarrow \mathbb{R}$  is a pre-specified objective function. As  $Y_i(0), Y_i(1)$  are never observed simultaneously, the joint distribution of  $(Y_i(0), Y_i(1), Z_i)$ , i.e.,  $\mu$ , is not identifiable. As a result, causal estimands (4) may also not be identifiable from observed data, i.e., two different joint distributions can yield different values of the causal estimand while producing the same distribution over observable quantities. This issue is commonly known as *partial identification*. For partially identifiable causal estimands, point estimation is infeasible, and

the object of interest becomes the partial identification (PI) set, that is, the set of values consistent with the identifiable marginal distributions of  $(Y_i(0), Z_i(0))$  and  $(Y_i(1), Z_i(1))$ , which we denote as

$$\begin{aligned} \Pi_c(P, Q) \triangleq \{ \pi \in \mathcal{P}(\mathcal{Y}^2 \times \mathcal{Z}) : \\ \pi_{Y(0), Z} = P, \pi_{Y(1), Z} = Q \}. \end{aligned} \quad (5)$$

Given a measurable function  $h$ , the PI set for the moment  $\mathbb{E}_\mu[h(Y(0), Y(1))]$  is

$$\{ \mathbb{E}_\pi[h(Y(0), Y(1))] : \pi \in \Pi_c(P, Q) \} = [V_c, \tilde{V}_c], \quad (6)$$

where we use the fact that the coupling set  $\Pi_c$  in (5) is convex and thus the induced PI set in (6) is a convex subset of  $\mathbb{R}$  and hence an interval<sup>1</sup>. Therefore, characterizing the PI set reduces to computing its lower and upper bounds. In particular, we focus on the lower bound

$$V_c = \min_{\pi \in \Pi_c(P, Q)} \mathbb{E}_\pi[h(Y(0), Y(1))], \quad (7)$$

which can be interpreted as a *conditional optimal transport* problem. The upper bound  $\tilde{V}_c$  is obtained analogously by replacing  $h$  with  $-h$ .

**Definition 2.1** (Conditional optimal transport). For a measurable objective function  $h$  and  $P, Q$  that satisfy  $P_Z = Q_Z$ , the conditional optimal transport between  $P, Q$  with respect to  $Z$  is defined as

$$CW_h(P, Q) = \min_{\pi \in \Pi_c(P, Q)} \mathbb{E}_\pi[h(Y(0), Y(1))].$$

For  $h = \|y_0 - y_1\|_2^p$ , we denote  $CW_p(P, Q) := (CW_h(P, Q))^{\frac{1}{p}}$ .

## 2.2 Curse of Dimensionality and Wavelet Density Estimator

It is well known that empirical estimation of optimal transport values such as  $V_c$  suffers from the curse of dimensionality of the outcome, even in the absence of covariates (e.g., [12]). This phenomenon is intrinsic to plug-in estimators. In particular, in the primal approach, replacing  $P$  and  $Q$  with the corresponding empirical distributions typically yields a statistical error of order  $n^{-1/d_Y}$ , which deteriorates rapidly as the dimension of the outcome space increases. In the conditional optimal transport literature, existing approaches (e.g., [29, 30]) additionally depend on the covariate dimension, leading to even slower convergence rates of order  $n^{-1/(d_Y + d_Z)}$  for estimating  $V_c$ .

In this paper, we exploit smoothness properties of the underlying data-generating distributions to mitigate the curse of dimensionality. Our approach is based on a wavelet expansion of the joint densities. For this purpose, we introduce the definition of the Besov space.

**Definition 2.2** (Besov space). Let  $s > 0$  and  $p, q \in [1, \infty]$ . Let  $\Psi = (\Phi, \Psi_1, \Psi_2, \dots)$  be a wavelet system on  $[0, 1]^d$ , where  $\Phi$  denotes the collection of scaling functions and  $\Psi_j$  the collection of wavelet functions at resolution level  $j$ . Let  $j_0 \geq 0$  denote a fixed coarse resolution level determined by the wavelet construction.

For  $f \in L^p([0, 1]^d)$  admitting the wavelet expansion

$$\begin{aligned} f(x) &= \sum_{\zeta \in \Phi} \theta_\zeta \zeta(x) + \sum_{j=j_0}^{\infty} \sum_{\xi \in \Psi_j} \theta_\xi \xi(x), \\ \theta_\zeta &= \int_{[0, 1]^d} \zeta(x) f(x) dx, \quad \theta_\xi = \int_{[0, 1]^d} \xi(x) f(x) dx, \end{aligned}$$

the Besov norm  $\|f\|_{\mathcal{B}_{p,q}^s([0, 1]^d)}$  is defined as

$$\|(\theta_\zeta)_{\zeta \in \Phi}\|_{\ell_p} + \left\| \left( 2^{j(s+d/2-d/p)} \|(\theta_\xi)_{\xi \in \Psi_j}\|_{\ell_p} \right)_{j \geq j_0} \right\|_{\ell_q}.$$

<sup>1</sup>The interval may be unbounded, with endpoints in  $\{-\infty, +\infty\}$ .

The Besov space  $\mathcal{B}_{p,q}^s([0,1]^d)$  is defined as

$$\left\{ f \in L^p([0,1]^d) : \|f\|_{\mathcal{B}_{p,q}^s([0,1]^d)} < \infty \right\}.$$

The Besov norm can be extended to negative smoothness indices  $s < 0$  via duality:

$$\mathcal{B}_{p',q'}^s([0,1]^d) = (\mathcal{B}_{p,q}^{-s}([0,1]^d))^*, \quad \frac{1}{p'} + \frac{1}{p} = 1, \quad \frac{1}{q'} + \frac{1}{q} = 1.$$

In this paper, we choose the boundary-corrected wavelet system on  $[0,1]^{d_Y+d_Z}$  and defer the details of this wavelet system to Section B. The reason why the wavelet expansion is useful for the analysis arises from the following result.

**Proposition 2.1** ([37, Theorem 4]). *Suppose that  $\hat{\mu}, \mu \in \mathcal{P}_{\text{ac}}([0,1]^d)$  with densities  $\hat{f}, f \in L^2([0,1]^d)$ . If  $f(x) \geq \gamma^{-1} \forall x \in [0,1]^d$  for some  $\gamma > 0$ , then there is a universal constant  $C_0 > 0$  such that*

$$W_2(\hat{\mu}, \mu) \leq C_0 \gamma^{\frac{1}{2}} \|\hat{f} - f\|_{\mathcal{B}_{2,1}^{-1}([0,1]^d)}.$$

**Definition 2.3** (Wavelet density estimator). Let  $J_n \geq j_0$  be a resolution level. Given i.i.d. observations  $(X_i)_{i=1}^n$  with density  $f$ , define the wavelet projection

$$\tilde{f}_{J_n}(x) := \sum_{\zeta \in \Phi} \hat{\theta}_\zeta \zeta(x) + \sum_{j=j_0}^{J_n} \sum_{\xi \in \Psi_j} \hat{\theta}_\xi \xi(x),$$

where  $\hat{\theta}_\zeta := \frac{1}{n} \sum_{i=1}^n \zeta(X_i)$ ,  $\hat{\theta}_\xi := \frac{1}{n} \sum_{i=1}^n \xi(X_i)$ .

The boundary-corrected wavelet density estimator is defined as

$$\hat{f}_{J_n}(x) = \frac{\tilde{f}_{J_n}(x) \mathbf{1}\{\tilde{f}_{J_n}(x) \geq 0\}}{\int_{\tilde{f}_{J_n}(x) \geq 0} \tilde{f}_{J_n}(x) dx}. \quad (8)$$

Specifically, in this work, we take  $J_n = \lfloor \frac{\log_2(n)}{2s+d_Y+d_Z} \rfloor$  and  $j_0 \geq \lfloor \log_2(s/0.18 + 1) \rfloor + 1$  (which is standard as discussed in [32, Section A.2]).

Additional to a wavelet expansion, we also focus on density with uniform smoothness described by the Hölder norm.

**Definition 2.4** (Hölder space). Let  $s > 0$ , the Hölder space  $C^s([0,1]^d)$  consists of functions  $f$  whose derivatives up to order  $\lfloor s \rfloor$  extend continuously to  $[0,1]^d$  and satisfy

$$\|f\|_{C^s([0,1]^d)} := \sum_{|\alpha| \leq \lfloor s \rfloor} \|D^\alpha f\|_\infty + \sum_{|\alpha| = \lfloor s \rfloor} \sup_{\substack{x,y \in [0,1]^d \\ x \neq y}} \frac{|D^\alpha f(x) - D^\alpha f(y)|}{\|x - y\|^{s - \lfloor s \rfloor}} < \infty,$$

where  $D^\alpha f = \frac{\partial^{|\alpha|} f}{\partial x_1^{\alpha_1} \dots \partial x_d^{\alpha_d}}$ ,  $|\alpha| = \sum_{i=1}^d \alpha_i$ .

To conclude this section, we present the following result, showing that any smooth density function embeds into the Besov space, admitting a wavelet expansion.

**Proposition 2.2** (c.f., [32, Lemma 25]).  $C^s([0,1]^d) \subseteq \mathcal{B}_{\infty,\infty}^s([0,1]^d)$ ,  $C^s \subseteq \mathcal{B}_{2,2}^{s-\epsilon}$  for any  $\epsilon > 0$ .

## 2.3 Assumption

**Assumption 2.1** (Bounded density). *Assume  $P, Q \in \mathcal{P}_{\text{ac}}([0,1]^{d_Y+d_Z})$ , and  $\gamma^{-1} \leq p, q \leq \gamma$  for  $\gamma > 0$ .*

**Assumption 2.2** (Smoothness). *Assume that, for a fixed smoothness parameter  $s > 0$ , the densities  $p, q \in C^{s+\epsilon}([0,1]^{d_Y+d_Z})$  for some  $\epsilon > 0$ .*

**Assumption 2.3** (Lipschitz objective). *The objective function  $h$  is  $L_h$ -Lipschitz, i.e.,  $|h(y_0) - h(y_1)| \leq L_h \|y_0 - y_1\|_2$ ,  $\forall y_0, y_1 \in [0, 1]^{d_Y}$ .*

Assumption 2.1 postulates that the density is bounded away from zero, a condition that is both standard and practically mild in nonparametric optimal transport. When this assumption is violated, the convergence rate of optimal transport estimators is known to change qualitatively; see [37, Section 5] for a detailed discussion.

Assumption 2.2 imposes smoothness on the density, which is central to our analysis. This regularity enables a wavelet-based representation of the density and is crucial for constructing estimators that are statistically more efficient than a direct plug-in approaches. Note that, for technical reasons, we require the density to possess slightly higher smoothness than  $s$ , namely  $s + \epsilon$  for an arbitrarily small  $\epsilon > 0$ .

Assumption 2.3 imposes the Lipschitz continuity of  $h$ , which is natural in optimal transport, as it guarantees stability of the optimal transport value with respect to perturbations of the input measures; see [42].

## 3 Main Result

### 3.1 Wavelet-based COT Estimator

In this section, we introduce the wavelet-based COT estimator, which is established upon the wavelet density estimator with alignment on the marginal density of  $Z$ .

**Definition 3.1** (Wavelet-based COT estimator). Suppose there is an i.i.d. sample  $\mathcal{S}_0 = ((Y_i(0), Z_i(0)), 1 \leq i \leq n)$  drawn  $P$  and an i.i.d. sample  $\mathcal{S}_1 = ((Y_j(1), Z_j(1)), 1 \leq j \leq n)$  drawn from  $Q$ ,  $\mathcal{S}_0$  independent of  $\mathcal{S}_1$ . Let the resolution level be  $J_n = \lfloor \frac{\log_2(n)}{2s+d_Y+d_Z} \rfloor$ .

- (i) Let  $\widehat{P}_n \in \mathcal{P}([0, 1]^{d_Y+d_Z})$  be the distribution associated with the wavelet density estimator based on  $\mathcal{S}_0$  (see Definition 2.3), and  $\widehat{Q}_n$  is defined similarly based on  $\mathcal{S}_1$ .
- (ii) Further, let  $\widehat{R}_n = (\widehat{P}_{n,Z} + \widehat{Q}_{n,Z})/2 \in \mathcal{P}([0, 1]^{d_Z})$ .
- (iii) Let  $\widehat{P}_n^\dagger(dy, dz) = \widehat{P}_{n,Y}^z(dy) \widehat{R}_n(dz)$ ,  $\widehat{Q}_n^\dagger(dy, dz) = \widehat{Q}_{n,Y}^z(dy) \widehat{R}_n(dz)$ . The wavelet-based COT estimator is defined by

$$\widehat{V}_{c,n} := CW_h(\widehat{P}_n^\dagger, \widehat{Q}_n^\dagger).$$

Since conditional optimal transport requires alignment of the  $Z$ -marginal, we construct a shared  $Z$ -marginal using the pooled  $Z$ -samples from both data sources. The paired  $(Y, Z)$  observations from each source are then used to estimate the corresponding conditional distributions.

Note that  $\widehat{P}_n^\dagger$  and  $\widehat{Q}_n^\dagger$  are continuous distributions. Consequently,  $\widehat{V}_{c,n}$  is approximated via a resampling procedure, which is standard in the literature (see, e.g., [46, 7]). The detailed algorithm is deferred to Section D.1.

In contrast to [25], our wavelet-based estimator does not require any cross-fitting and thus avoids the repeated computation across folds as well as the artificial randomness introduced by sample splitting.

### 3.2 Fast Convergence Rate with General Objective

To bound the statistical convergence rate of the wavelet-based COT estimator, we first present the following stability result of COT under Lipschitz kernels and objectives.

**Proposition 3.1** (Stability). *Suppose that  $W_1(P_Y^z, P_Y^{z'}) \leq L_p \|z - z'\|_2$ ,  $W_1(Q_Y^z, Q_Y^{z'}) \leq L_p \|z - z'\|_2$  for any  $z, z'$ , and  $h$  is  $L_h$ -Lipschitz, then*

$$|CW_h(\widehat{P}, \widehat{Q}) - CW_h(P, Q)| \leq 2L_h L_p W_1(P_Z, \widehat{P}_Z) + L_h \int W_1(P_Y^z, \widehat{P}_Y^z) + W_1(Q_Y^z, \widehat{Q}_Y^z) d\widehat{P}_Z(z). \quad (9)$$

Table 1: Comparison of statistical convergence rates for COT value estimation.

Reference	Estimation Rate	Key Assumptions
[30]	$n^{-\frac{1}{2\sqrt{d_Y+d_Z}}}$	Lipschitz kernel
[25]	$n^{-1/2}$	Density, optimal dual are estimated at rate $O(n^{-1/4})$
<b>This work</b>	$n^{-\frac{s}{2s+d_Y+d_Z}}$	Densities in $\mathcal{C}^{s+\epsilon}$ , bounded away from zero
<b>This work</b>	$n^{-\frac{2s}{2s+d_Y+d_Z}} \vee n^{-1/2}$	Densities in $\mathcal{C}^{s+\epsilon}$ , bounded away from zero, $h$ quadratic

The first term on the right-hand side of (9) can be bounded using standard results from wavelet density estimation [37]. In contrast, we derive the convergence rate of the second term for the density estimator introduced in Section 3.1.

**Proposition 3.2** (Key estimation bound). *Under Assumption 2.1-2.2,*

$$\mathbb{E} \left[ \int W_2^2(\widehat{Q}_Y^z, Q_Y^z) \widehat{R}(dz) \right] \leq C n^{-\frac{2s}{2s+d_Y+d_Z}},$$

where  $C$  is a constant that depends on  $P, Q, \gamma, s, d_Y, d_Z$ .

We are now ready to state our main result.

**Theorem 3.1** (Fast convergence of COT under smooth densities). *Under Assumption 2.1 ( $\gamma$ ), 2.2 ( $s$ ) and 2.3 ( $L_h$ ),*

$$\mathbb{E}[|V_c - \widehat{V}_{c,n}|] \leq C L_h n^{-\frac{s}{2s+d_Y+d_Z}},$$

where  $C$  is a constant that depends on  $P, Q, \gamma, s, d_Y, d_Z$ .

When  $s$  is sufficiently large, the convergence rate of the COT estimator is close to the parametric rate of order  $n^{-1/2}$ , relieving the dependence of dimension  $d_Y + d_Z$ . To conclude this section, we compare the rate and assumption of our method with other existing approach estimating the COT value that has a finite-sample convergence rate; see Table 1.

### 3.3 Statistical Inference with Quadratic Objective

In this section, we focus on the quadratic objective  $h(y_0, y_1) = \|y_0 - y_1\|_2^2$ , which allows a stronger stability bound and thus an analysis of the asymptotic distribution of the wavelet-based COT estimator, enabling standard statistical inference. The results below readily extend to any objective  $h(y_0, y_1) = y_0^\top M y_1$  with  $M \in \mathbb{R}^{d_Y \times d_Y} \succeq 0$ .

When the objective function is quadratic for an optimal transport problem, Brenier's theorem [26, 6] shows that the optimal solution is a map defined as the gradient of the so-called Brenier potential function. In our conditional setting, we let  $\varphi(y, z)$  be the Brenier potential between  $P_Y^z$  and  $Q_Y^z$  for each  $z \in [0, 1]^{d_Z}$ . To obtain a sharper convergence-rate analysis than in the previous section, we will impose stronger smoothness assumptions on the densities  $p, q$  and the functions  $\varphi$ . In particular, under a quadratic objective  $h$ , the smoothness of  $\varphi$  can often be deduced from that of  $p$  and  $q$ . Roughly speaking, for each fixed  $z$ , if the conditional densities  $p_Y^z(y)$  and  $q_Y^z(y) \in \mathcal{C}^s([0, 1]^{d_Y})$ , then typically the corresponding potentials  $\varphi(\cdot, z) \in \mathcal{C}^{s+2}([0, 1]^{d_Y})$ , under suitable regularity and boundary conditions. See, for instance, [43, Chapter 12].

**Proposition 3.3** (Stability with quadratic objective). *Under Assumption 2.1 ( $\gamma$ ), and further assume that*

- (i)  $\varphi(\cdot, z) \in \mathcal{C}^2([0, 1]^{d_Y})$  for any  $z \in [0, 1]^{d_Z}$ .
- (ii)  $C_2 := \sup_{z \in [0, 1]^{d_Z}} \|\varphi(\cdot, z)\|_{\mathcal{C}^2([0, 1]^{d_Y})} < \infty$ .

Then there exists a constant  $\lambda > 0$  that depends on  $\gamma, C_2$  such that

$$\begin{aligned} 0 &\leq CW_2(\widehat{P}_n^\dagger, \widehat{Q}_n^\dagger)^2 - CW_2(P, Q)^2 - \int \phi d(\widehat{P}_n^\dagger - P) - \int \psi d(\widehat{Q}_n^\dagger - Q) \\ &\leq 2\lambda \int W_2^2(\widehat{P}_Y^z, P_Y^z) + W_2^2(\widehat{Q}_Y^z, Q_Y^z) \widehat{R}_n(dz), \end{aligned}$$

where  $\phi(y, z) = \|y\|_2^2 - \varphi(y, z)$  and  $\psi(y, z) = \|y\|_2^2 - \varphi^*(y, z)$ , with  $\varphi^*(y, z) := \sup_{y' \in [0, 1]^{d_Y}} \{y^\top y' - \varphi(y', z)\}$ .

When  $s$  is sufficiently large, the right-hand side of the above inequality is of order  $o_p(n^{-1/2})$ , as implied by Eq. (9) and Theorem 3.1. Thus, the target converges to the distributional limit of  $\int \phi d(\widehat{P}_n^\dagger - P) + \int \psi d(\widehat{Q}_n^\dagger - Q)$ . As a result, we have the following result.

**Theorem 3.2.** *Under Assumption 2.1 ( $\gamma$ ) - 2.2 ( $s$ ), and that  $p, q, \varphi \in \mathcal{C}^{s+1}([0, 1]^{d_Y+d_Z})$ ,  $2s > d_Y + d_Z$ ,*

$$\sqrt{n} \left( CW_2^2(\widehat{P}_n^\dagger, \widehat{Q}_n^\dagger) - CW_2^2(P, Q)^2 \right) \xrightarrow{d} \mathcal{N}(0, \sigma^2),$$

where  $\sigma^2 := 2(\text{Var}_P(\eta(Y, Z)) + \text{Var}_Q(\kappa(Y, Z)))$  with

$$\begin{aligned} \eta(y, z) &:= \phi(y, z) - \frac{1}{2} \left( \int \left( \phi(y', z) \frac{p(y', z)}{p_Z(z)} - \psi(y', z) \frac{q(y', z)}{q_Z(z)} \right) dy' \right), \\ \kappa(y, z) &:= \psi(y, z) - \frac{1}{2} \left( \int \left( \psi(y', z) \frac{q(y', z)}{q_Z(z)} - \phi(y', z) \frac{p(y', z)}{p_Z(z)} \right) dy' \right). \end{aligned}$$

A key step in proving Theorem 3.2 is to establish a central limit theorem for

$$\int \phi d(\widehat{P}_n^\dagger - P) + \int \psi d(\widehat{Q}_n^\dagger - Q).$$

Although  $\widehat{P}_n^\dagger$  and  $\widehat{Q}_n^\dagger$  are dependent through the shared estimator  $\widehat{R}$  (thus the argument in [31] cannot be applied directly), the identity  $\widehat{r} - \widehat{p} = (\widehat{q} - \widehat{p})/2$  allows a decomposition that yields the desired CLT; see Section C.4.

**Remark 3.1** ( $d_Z = 0$ ). When there is no covariate, the central limit theorem can be derived with milder assumption. For example, for  $d_Y = 1$ , [8] shows the CLT of the plug-in estimator (using the empirical distribution) when  $p, q \in \mathcal{C}^1([0, 1])$ ; [32] extends the CLT of wavelet-based estimator for general  $d_Y$  when  $p, q \in \mathcal{C}^s([0, 1]^{d_Y})$ ,  $s > d_Y/2 - 2$ . By contrast, this work extends it to a more general result with covariate and identifies a similar smoothness condition  $s > (d_Y + d_Z)/2$ .

**Remark 3.2** ( $P = Q$ ). The asymptotic variance  $\sigma^2$  is positive if and only if the conditional distributions  $P_{Y|Z}$  and  $Q_{Y|Z}$  differ on a set of  $z$  with positive probability. When the two conditional distributions coincide, i.e.,  $P_{Y|Z} = Q_{Y|Z}$ , the conditional Wasserstein distance is zero, and  $CW_2^2(\widehat{P}_n^\dagger, \widehat{Q}_n^\dagger)$  converges to zero faster than the order of  $n^{-1/2}$ .

**Remark 3.3** (Asymptotic variance estimation). The asymptotic variance  $\sigma^2$  in Theorem 3.2 can be consistently estimated using plug-in estimators of the conditional potential functions. When these quantities are difficult to estimate, subsampling-based approaches, particularly the bootstrap, can be used to approximate the variance and construct confidence intervals.

## 4 Numerical Experiment

The code and data are available at [https://github.com/siruilin1998/causalOT\\_inference](https://github.com/siruilin1998/causalOT_inference).

### 4.1 Estimation

We empirically compare the convergence rate of our estimator (Section 3.3) with existing approaches including [25, 29, 30].

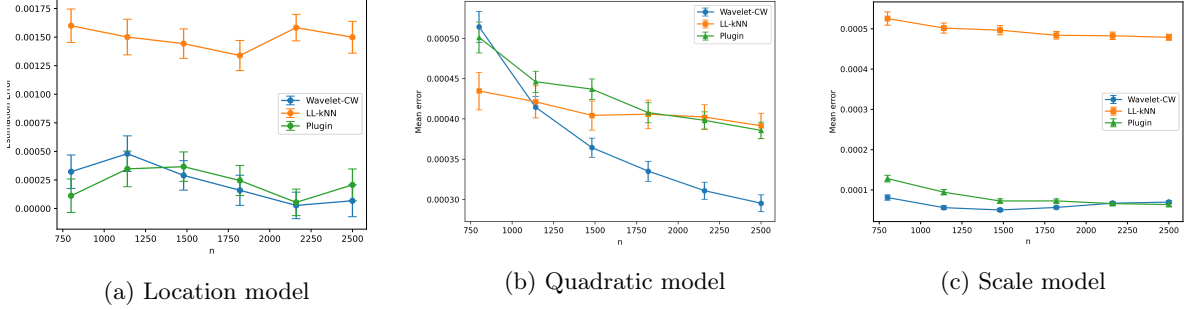


Figure 1: Plots of estimation error comparison of our method (*Wavelet CW estimate*) with [25] (*LL-kNN*, for which we use ‘knn’-based nuisance estimator) and [30] (*Plugin*) with  $d_Y = 1$ ,  $d_Z = 1$ . The estimation error is defined by  $\mathbb{E}[|V_c - \widehat{V}_c|]$ . The mean error curve and the corresponding standard-error confidence bands are computed by aggregating results over 100 Monte Carlo repetitions. The plots show that the convergence rate of our method is at least comparable with the existing approaches in low dimension.

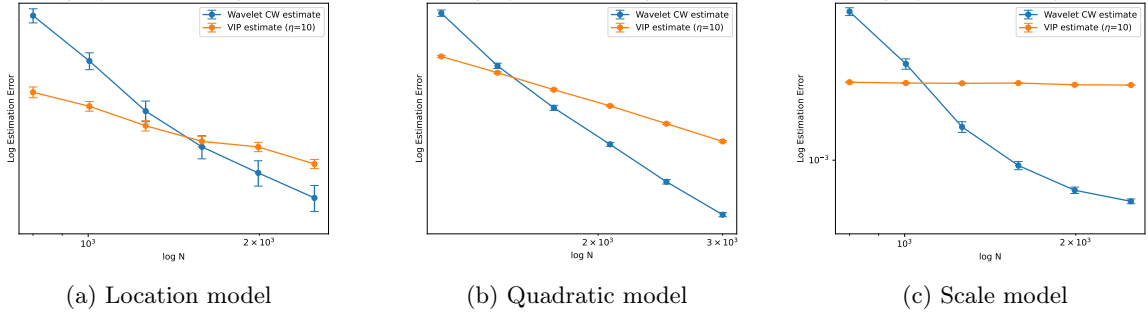


Figure 2: Log-log plots of estimation error comparison of our method (*Wavelet CW estimate*) and [29] (*VIP estimate* with  $\eta = 10$ ) with  $d_Y = 2$ ,  $d_Z = 2$ . The estimation error is defined by  $\mathbb{E}[|V_c - \widehat{V}_c|]$ . The mean error curve and the corresponding standard-error confidence bands are computed by aggregating over 300 Monte Carlo repetitions. The plots show that the convergence rate of our method is significantly faster than the rate of VIP estimate, which suffers from the curse of dimensionality based on its theory.

**Data generation mechanism.** We outline a default data-generating mechanism. Each dimension of the covariate  $Z \in [0, 1]^{d_Z}$  are drawn i.i.d. from  $\text{Uniform}(0, 1)$ . The potential outcomes  $Y$  are drawn from

$$Y(w) \mid Z = z \sim \mathcal{N}(\mu_w(z), \Sigma_w(z)), \quad w \in \{0, 1\}.$$

The objective function is quadratic,  $h = \|y_0 - y_1\|_2^2$ . This underlying distribution and objective enable a closed form evaluation of the COT value thanks to the Gelbrich formula (Proposition A.1). Note that we shall choose the parameter  $\mu_w(z), \Sigma_w(z)$  appropriately such that most of its measure is supported on  $[0, 1]^{d_Y}$ .

Specifically, we consider three data models.

1. (Location model)  $\mu_w(z) = \alpha_w z + \beta_w$ ,  $\Sigma_w(z) \equiv \Sigma_w$ .
2. (Quadratic model)  $\mu_w(z) = A_w(z - \alpha_w)^2 + \beta_w$ ,  $\Sigma_w(z) \equiv \Sigma_w$ , where  $(z - \alpha_w)^2$  is an entry-wise square.
3. (Scale model)  $\mu_w(z) \equiv \alpha_w$ ,  $\Sigma_w(z) = (\zeta_w^\top z) \times \Sigma_w$ , where  $(\zeta_w^\top z)$  is a scalar.

**Implementation.** We implement our method following Algorithm 1, Algorithm 2 with the wavelet estimator parameters specified in Section E. The method [25] is implemented using `DualBounds`<sup>2</sup>. The methods from [29, 30] are implemented using the public code they upload with the paper.

<sup>2</sup><https://dualbounds.readthedocs.io/en/latest/index.html>

Table 2: Coverage of the proposed 95% confidence intervals across different settings. We consider three choices of  $(d_Y, d_Z)$ , each evaluated at three sample sizes. Confidence intervals are constructed using the bootstrap with 100 resamples. Reported coverage rates are aggregated over 200 Monte Carlo repetitions.

Dimension	$d_Y = 2, d_Z = 1$			$d_Y = 2, d_Z = 2$			$d_Y = 3, d_Z = 2$		
Sample size ( $n$ )	1000	2000	3000	1000	2000	3000	4000	5000	6000
Coverage	92.5%	93%	93.5%	86%	98.5%	97.5%	90%	93.5%	96%

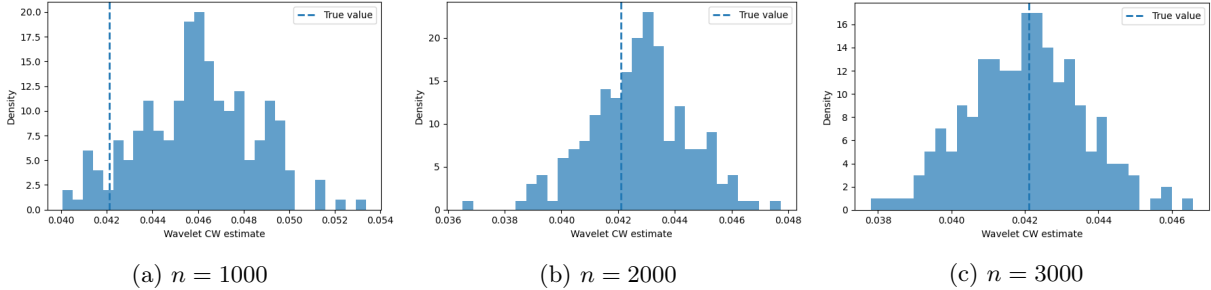


Figure 3: Histogram of the proposed estimator with the true value marked by a vertical dashed line. Here the default setting  $d_Y = 2, d_Z = 2$  is adopted. The results are aggregated over 200 Monte Carlo repetitions.

**Case i.** ( $d_Y = 1$ ) We first compare our method with [25] and [30] in the setting of  $d_Y = d_Z = 1$  across the three models. Specifically, for [25], we use the knn-based (nonparametric) nuisance estimator to avoid model misspecification. The plots of estimation error comparison are shown in Figure 1. The plots imply that in low-dimensional cases, our method performs comparably to existing approaches, consistent with the fact that smoothness assumptions do not improve convergence rates beyond the parametric regime.

**Case ii.** ( $d_Y > 1$ ) Since neither the approach of [25] nor [30] is implemented for  $d_Y > 1$ , we focus on comparing with the VIP estimate of [29], for which we take  $\eta = 10$  so that the estimator is asymptotically unbiased. The log-log plots of the estimation error comparison of these two methods are shown in Figure 2. The plots demonstrate a significant improvement of convergence rate of our method comparing to the VIP estimate across multiple scenarios, which is due to the structure of our wavelet estimator that leverages the smoothness of the underlying density functions.

## 4.2 Inference

We empirically validate the performance of inference of our proposal. In particular, we focus on the case  $d_Y > 1$ , where standard methods such as quantile-based approaches are not applicable.

**Data generation mechanism.** We use the location model to evaluate the inference performance. Specifically, we consider a total of three scenarios with different dimensions:  $(d_Y = 2, d_Z = 1)$ ,  $(d_Y = 2, d_Z = 2)$  as the default setting, and  $(d_Y = 3, d_Z = 2)$ . The details of  $\mu_w(z)$ ,  $\Sigma_w(z)$  are provided in Section E.2. For each scenario, we consider three different sample sizes  $n$ , and the specific values are listed in Table 2.

**Bootstrap.** We use the bootstrap with 100 resamples to estimate the variance  $\sigma^2$  in Theorem 3.2 and plug it in to construct the confidence interval. The alternative approach for  $d_Y > 1$  discussed in Section 4.1 either has non-negligible bias or lacks an established asymptotic distribution, making it unsuitable for statistical inference. We therefore focus on our method.

**Coverage rate.** We report the coverage results for 95% confidence intervals in Table 2. Overall, the coverage rates are acceptable when the sample size  $n$  is moderately large. As expected, for each configuration

of  $(d_Y, d_Z)$ , coverage improves as the sample size increases; as the dimensions  $d_Y$  and  $d_Z$  grow, larger samples are required to achieve proper coverage.

**Asymptotic distribution.** In Figure 3, we display the distribution of the proposed estimator  $CW_2^2(\hat{P}_n^\dagger, \hat{Q}_n^\dagger)$ , with the true value  $CW_2^2(P, Q)$  marked by a vertical dashed line. We focus on the default setting  $d_Y = 2$ ,  $d_Z = 2$ ; histograms for the other two settings are provided in Section E. The distribution of the estimator  $CW_2^2(\hat{P}_n^\dagger, \hat{Q}_n^\dagger)$  becomes increasingly normal as  $n$  grows, consistent with the CLT in Theorem 3.2. The bias also decreases with larger sample sizes: for  $n = 1000$ , the estimator is upward biased, while by  $n = 3000$ , the bias becomes negligible.

### 4.3 Real Data Analysis

We investigate the randomized experiment from the Student Achievement and Retention Project (STAR) [1], which evaluated the effects of academic support services and financial incentives on college student performance. We use gender and baseline GPA (supported on  $[0, 4]$ ) as covariates, and first-year and second-year GPA (supported on  $[0, 4]$ ) as outcomes. Because the true treatment effect is not directly observable, we construct hypothetical potential outcomes under control and treatment based on the observed outcomes. Specifically, we treat the original outcomes as control potential outcomes and generate gender-dependent treatment effects, motivated by the finding in [1] that female students benefit more from the intervention. We add these treatment effects to the control outcomes to obtain treatment potential outcomes. Based on the constructed hypothetical dataset, in each simulation replicate, we randomly sample 1300 control and 1300 treatment observations and use them as the observed dataset. We generate 200 datasets and aggregate the results.

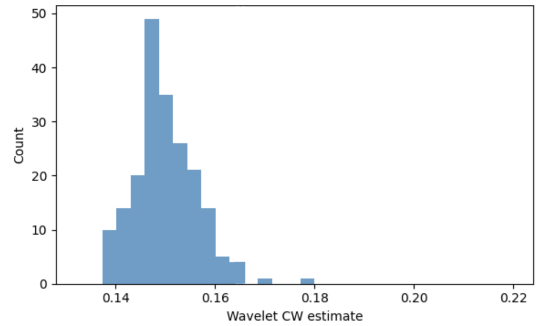
We apply our method to each generated dataset as described in Section 4.2, with outcome dimension  $d_Y = 2$  and covariate dimension  $d_Z = 1$  or 2. Particularly, we consider three sets of covariates for conditioning:

- (a) Conditioning on baseline GPA only.
- (b) Conditioning on gender only.
- (c) Conditioning on baseline GPA and gender.

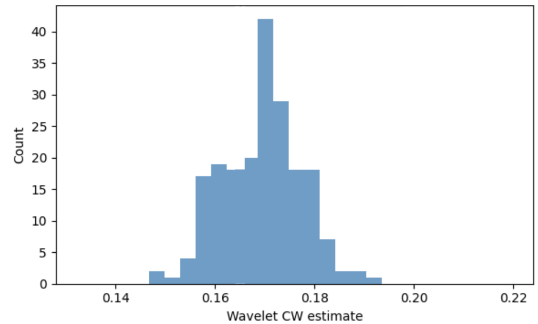
By the construction of our hypothetical treatment effects, the conditional distribution under treatment differs from that under control by a location shift depending on the gender. Therefore, conditioning on gender, either alone or together with the baseline GPA, the optimal values of the population-wise COT recover the sharp lower bound given by the Cauchy-Schwarz inequality,

$$\mathbb{E} \left[ \left\| \mathbb{E}[Y(1) \mid \text{Gender}] - \mathbb{E}[Y(0) \mid \text{Gender}] \right\|_2^2 \right].$$

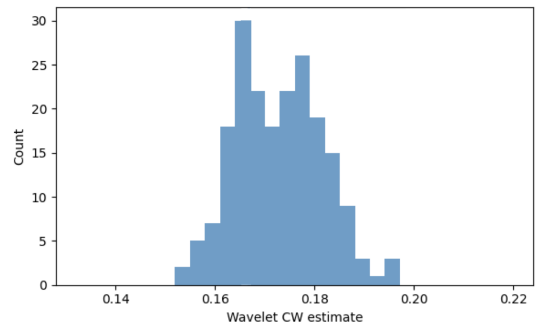
In contrast, when conditioning only on baseline GPA, the conditioning set does not fully capture the treatment effect heterogeneity, and therefore the optimal value of the COT is strictly smaller, leading to a looser PI set.



(a) Conditioning on baseline GPA only



(b) Conditioning on gender only



(c) Conditioning on baseline GPA and gender

Figure 4: Histogram of the proposed estimator applied to hypothetical STAR datasets under different conditioning sets of covariates. Results are aggregated over 200 simulated hypothetical datasets.

As shown in Figure 4, when conditioning on gender (panels (b) and (c)), the estimators’ distributions are centered at similar values, both substantially larger than when conditioning only on baseline GPA (panel (a)). This is consistent with the theoretical discussion above and highlights the importance of conditioning on informative covariates to tighten the partial identification sets. When conditioning on both gender and baseline GPA (panel (c),  $d_Z = 2$ ), the estimator exhibits slightly slower convergence, resulting in mildly larger upward bias and a less normal distribution compared to conditioning on gender alone (panel (b),  $d_Z = 1$ ). One possible future direction is to combine the proposed method with automatic selection of influential covariates.

## 5 Discussion and Conclusion

We propose a primal COT solver that leverages the smoothness of the marginal density to enable accurate estimation and statistical inference for causal partial identification sets. Our method accommodates multivariate outcomes, which are not supported by existing quantile-based approaches, and relieves the curse of dimensionality faced by alternative methods. Methodologically, we establish stability results for both general and quadratic objective functions, for a procedure that incorporates a tailored alignment of the covariate marginal distribution. Empirically, our estimator converges faster than competitors and achieves desirable coverage for moderately large sample sizes.

We outline one future direction. The direction is to extend the framework to more complex experimental designs where the probability of receiving treatment (propensity score) depends on the covariates. This extension would be useful for handling observational studies under the ignorability assumption, where treatment assignment is not randomized but can be modeled using a covariate-dependent propensity score.

## References

- [1] Angrist, J., Lang, D., and Oreopoulos, P. “Incentives and services for college achievement: Evidence from a randomized trial”. In: *American Economic Journal: Applied Economics* 1.1 (2009), pp. 136–163.
- [2] Arjovsky, M., Chintala, S., and Bottou, L. “Wasserstein generative adversarial networks”. In: *International Conference on Machine Learning*. PMLR. 2017, pp. 214–223.
- [3] Backhoff, J. et al. “Estimating processes in adapted Wasserstein distance”. In: *The Annals of Applied Probability* 32.1 (2022), pp. 529–550.
- [4] Basu, S., Kolouri, S., and Rohde, G. K. “Detecting and visualizing cell phenotype differences from microscopy images using transport-based morphometry”. In: *Proceedings of the National Academy of Sciences* 111.9 (2014), pp. 3448–3453.
- [5] Blanchet, J. and Murthy, K. “Quantifying distributional model risk via optimal transport”. In: *Mathematics of Operations Research* 44.2 (2019), pp. 565–600.
- [6] Brenier, Y. “Polar factorization and monotone rearrangement of vector-valued functions”. In: *Communications on Pure and Applied Mathematics* 44.4 (1991), pp. 375–417.
- [7] Deb, N., Ghosal, P., and Sen, B. “Rates of estimation of optimal transport maps using plug-in estimators via barycentric projections”. In: *Advances in Neural Information Processing Systems* 34 (2021), pp. 29736–29753.
- [8] Del Barrio, E., Giné, E., and Utzet, F. “Asymptotics for L2 functionals of the empirical quantile process, with applications to tests of fit based on weighted Wasserstein distances”. In: *Bernoulli* 11.1 (2005), pp. 131–189.
- [9] Fan, Y. and Park, S. S. “Sharp bounds on the distribution of treatment effects and their statistical inference”. In: *Econometric Theory* 26.3 (2010), pp. 931–951.
- [10] Fan, Y., Pass, B., and Shi, X. “Partial Identification in Moment Models with Incomplete Data via Optimal Transport”. In: *arXiv preprint arXiv:2503.16098* (2025).
- [11] Flamary, R. et al. “POT: Python optimal transport”. In: *Journal of Machine Learning Research* 22.78 (2021), pp. 1–8.

- [12] Fournier, N. and Guillin, A. “On the rate of convergence in Wasserstein distance of the empirical measure”. In: *Probability Theory and Related Fields* 162.3 (2015), pp. 707–738.
- [13] Galichon, A. *Optimal Transport Methods in Economics*. Princeton University Press, 2018.
- [14] Gao, Z., Ge, S., and Qian, J. “Bridging Multiple Worlds: Multi-Marginal Optimal Transport for Causal Partial-Identification Problem”. In: *Proceedings of the 28th International Conference on Artificial Intelligence and Statistics*. 2025.
- [15] Gelbrich, M. “On a formula for the  $L^2$  Wasserstein metric between measures on Euclidean and Hilbert spaces”. In: *Mathematische Nachrichten* 147.1 (1990), pp. 185–203.
- [16] Genevay, A., Peyré, G., and Cuturi, M. “Learning generative models with sinkhorn divergences”. In: *International Conference on Artificial Intelligence and Statistics*. PMLR. 2018, pp. 1608–1617.
- [17] Gigli, N. “On Hölder continuity-in-time of the optimal transport map towards measures along a curve”. In: *Proceedings of the Edinburgh Mathematical Society* 54.2 (2011), pp. 401–409.
- [18] Gulrajani, I. et al. “Improved training of Wasserstein GANs”. In: *Advances in Neural Information Processing Systems* 30 (2017).
- [19] Härdle, W. et al. *Wavelets, approximation, and statistical applications*. Vol. 129. Springer Science & Business Media, 2012.
- [20] Hosseini, B., Hsu, A. W., and Taghvaei, A. “Conditional optimal transport on function spaces”. In: *SIAM/ASA Journal on Uncertainty Quantification* 13.1 (2025), pp. 304–338.
- [21] Hundrieser, S. et al. “A unifying approach to distributional limits for empirical optimal transport”. In: *arXiv preprint* (2022). arXiv: [2202.12790](https://arxiv.org/abs/2202.12790).
- [22] Hütter, J.-C. and Rigollet, P. “Minimax Estimation of Smooth Optimal Transport Maps”. In: *The Annals of Statistics* 49.2 (2021), pp. 1166–1194. DOI: [10.1214/20-AOS1997](https://doi.org/10.1214/20-AOS1997).
- [23] Imbens, G. W. and Rubin, D. B. *Causal Inference in Statistics, Social, and Biomedical Sciences*. Cambridge university press, 2015.
- [24] Al-Jarrah, M. et al. “Error Analysis of Triangular Optimal Transport Maps for Filtering”. In: *arXiv preprint arXiv:2510.19283* (2025).
- [25] Ji, W., Lei, L., and Spector, A. “Model-agnostic covariate-assisted inference on partially identified causal effects”. In: *arXiv preprint* (2023). arXiv: [2310.08115](https://arxiv.org/abs/2310.08115).
- [26] Knott, M. and Smith, C. S. “On the optimal mapping of distributions”. In: *Journal of Optimization Theory and Applications* 43 (1984), pp. 39–49.
- [27] Kolouri, S. et al. “Optimal mass transport: Signal processing and machine-learning applications”. In: *IEEE Signal Processing* 34.4 (2017), pp. 43–59.
- [28] Kuhn, D. et al. “Wasserstein distributionally robust optimization: Theory and applications in machine learning”. In: *Operations research & management science in the age of analytics*. Informs, 2019, pp. 130–166.
- [29] Lin, S. et al. “Tightening Causal Bounds via Covariate-Aware Optimal Transport”. In: *Proceedings of the 42nd International Conference on Machine Learning*. 2025.
- [30] Lin, S. et al. “Causal Partial Identification via Conditional Optimal Transport”. In: *Proceedings of the Twenty-Ninth International Conference on Artificial Intelligence and Statistics (AISTATS)*. 2026.
- [31] Manole, T. et al. “Central Limit Theorems for Smooth Optimal Transport Maps”. In: *Proceedings of the 2023 IMS International Conference on Statistics and Data Science*. 2023, p. 323.
- [32] Manole, T. et al. “Plugin estimation of smooth optimal transport maps”. In: *Annals of Statistics* 52.3 (2024), pp. 966–998.
- [33] Manupriya, P. et al. “Consistent Optimal Transport with Empirical Conditional Measures”. In: *Proceedings of the 27th International Conference on Artificial Intelligence and Statistics*. 2024, pp. 3646–3654.
- [34] Meyer, Y. *Wavelets and operators*. 37. Cambridge university press, 1992.

- [35] Mohajerin Esfahani, P. and Kuhn, D. “Data-driven distributionally robust optimization using the Wasserstein metric: Performance guarantees and tractable reformulations”. In: *Mathematical Programming* 171.1 (2018), pp. 115–166.
- [36] Nguyen, V. A. et al. “Robustifying conditional portfolio decisions via optimal transport”. In: *Operations Research* (2024).
- [37] Niles-Weed, J. and Berthet, Q. “Minimax estimation of smooth densities in Wasserstein distance”. In: *The Annals of Statistics* 50.3 (2022), pp. 1519–1540.
- [38] Panaretos, V. M. and Zemel, Y. “Statistical aspects of Wasserstein distances”. In: *Annual Review of Statistics and its Application* 6 (2019), pp. 405–431.
- [39] Robert, C. P., Casella, G., and Casella, G. *Monte Carlo statistical methods*. Vol. 2. Springer, 1999.
- [40] Rubin, D. B. “Estimating causal effects of treatments in randomized and nonrandomized studies.” In: *Journal of Educational Psychology* 66.5 (1974), p. 688.
- [41] Rubner, Y., Tomasi, C., and Guibas, L. J. “The earth mover’s distance as a metric for image retrieval”. In: *International Journal of Computer Vision* 40.2 (2000), pp. 99–121.
- [42] Villani, C. *Topics in Optimal Transportation*. Vol. 58. American Mathematical Society, 2003.
- [43] Villani, C. *Optimal Transport: Old and New*. Vol. 338. Springer, 2008.
- [44] Villani, C. et al. *Optimal Transport: Old and New*. Vol. 338. Springer, 2009.
- [45] Wang, Z. O. et al. “Efficient neural network approaches for conditional optimal transport with applications in Bayesian inference”. In: *arXiv preprint* (2023). arXiv: [2310.16975](https://arxiv.org/abs/2310.16975).
- [46] Weed, J. and Berthet, Q. “Estimation of smooth densities in Wasserstein distance”. In: *conference on Learning Theory*. PMLR. 2019, pp. 3118–3119.
- [47] Xu, T. et al. “COT-GAN: Generating sequential data via causal optimal transport”. In: *Advances in Neural Information Processing Systems* 33 (2020), pp. 8798–8809.

## A Optimal Transport

**Definition A.1** (Optimal transport). Given a measurable objective function  $h$  and probability distributions  $P, Q \in \mathcal{P}(\mathbb{R}^{dx})$ , the OT distance is defined as

$$W_h(P, Q) \triangleq \min_{\pi \in \Pi(P, Q)} \mathbb{E}_\pi[h(X, X')],$$

where

$$\Pi(P, Q) \triangleq \{\pi \in \mathcal{P}(\mathcal{X}^2) : \pi_X = P, \pi_{X'} = Q\}. \quad (10)$$

When  $h(x, x') = \|x - x'\|_2^p$ , we denote  $W_p(P, Q) = W_h(P, Q)^{\frac{1}{p}}$ , which is the so-called Wasserstein  $p$ -distance.

The 2-Wasserstein distance between Gaussian measures admits a closed-form expression.

**Proposition A.1** (OT between Gaussian distributions [15]).

$$W_2^2(\mathcal{N}(m_0, \Sigma_0), \mathcal{N}(m_1, \Sigma_1)) = \|m_0 - m_1\|_2^2 + \text{tr}\left(\Sigma_0 + \Sigma_1 - 2(\Sigma_1^{1/2}\Sigma_0\Sigma_1^{1/2})^{1/2}\right).$$

## B Boundary-corrected Wavelet System

Next, we describe the specific wavelet basis used in our proposal.

**Definition B.1** (Boundary-corrected wavelet basis). Let  $j_0 \geq 0$  be the minimal resolution level at which boundary correction is applied. The boundary-corrected wavelet basis on  $L^2([0, 1])$  is defined by

$$\begin{aligned}\Phi_0^{\text{bc}} &= \{\phi_{j_0 k}^{\text{bc}}, k \in \mathcal{K}_0(j_0)\}, \\ \Psi_0^{\text{bc}} &= \{\psi_{jk}^{\text{bc}}, k \in \mathcal{K}_0(j), j \geq j_0\},\end{aligned}$$

where  $\mathcal{K}_0(j) := \{0, 1, \dots, 2^j - 1\}$ . Specifically, the wavelet basis is compactly supported orthonormal on  $[0, 1]$ . The concrete definition of  $\phi^{\text{bc}}, \psi^{\text{bc}}$  can be found in [32, Section A.2.1].

For outcomes  $y \in [0, 1]^{d_Y}$  and covariates  $z \in [0, 1]^{d_Z}$ , define

$$x = ((y_s)_{1 \leq s \leq d_Y}, (z_{s'})_{1 \leq s' \leq d_Z}) \in [0, 1]^{d_Y + d_Z}.$$

The tensor-product boundary-corrected wavelet functions on  $[0, 1]^{d_Y + d_Z}$  are defined by

$$\left\{ \begin{array}{l} \Phi_{j_0, \mathbf{k}}^{\text{bc}}(x) = \prod_{r=1}^{d_Y + d_Z} \phi_{j_0 k_r}^{\text{bc}}(x_r), \quad \mathbf{k} \in \mathcal{K}_0(j_0)^{d_Y + d_Z} \\ \Psi_{j, \mathbf{k}, \mathbf{l}}^{\text{bc}}(x) = \prod_{r=1}^{d_Y + d_Z} \begin{cases} \phi_{j, k_r}^{\text{bc}}(x_r), & l_r = 0, \\ \psi_{j, k_r}^{\text{bc}}(x_r), & l_r = 1, \end{cases} \quad \mathbf{l} \in \{0, 1\}^{d_Y + d_Z} \setminus \{(0, \dots, 0)\}, \mathbf{k} \in \mathcal{K}_0(j)^{d_Y + d_Z}, j \geq j_0 \end{array} \right\},$$

where  $\mathbf{k} = (k_1, \dots, k_{d_Y + d_Z})$  and  $\mathbf{l} = (l_1, \dots, l_{d_Y + d_Z})$ .

## C Additional Theoretical Results and Proofs

**Notation.** In the following sections, for simplicity, we will write  $\hat{P}_n$  (resp.  $\hat{Q}_n, \hat{R}_n$ ) as  $\hat{P}$  (resp.  $\hat{Q}, \hat{R}$ ).

In this section, we present the technical proof of the core result (Proposition C.1). As a preparation, we introduce the following lemmas.

**Lemma C.1** ([37, Theorem 4]). *Suppose that  $\hat{\mu}, \mu \in \mathcal{P}_{\text{ac}}([0, 1]^d)$ , and let  $\hat{f}, f \in L^2([0, 1]^d)$  be the density function of  $\hat{\mu}, \mu$ , respectively. If there exists a constant  $\gamma > 0$  such that  $\hat{f}(x) \vee f(x) \geq \gamma^{-1} \forall x \in [0, 1]^d$ , then*

$$W_2(\hat{\mu}, \mu) \leq C_{\text{wb}} \gamma^{\frac{1}{2}} \|\hat{f} - f\|_{\mathcal{B}_{2,1}^{-1}([0, 1]^d)},$$

where  $C_{\text{wb}} > 0$  is a universal constant.

**Lemma C.2** ([34, Section 6.10, Proposition 7]). *There is a universal constant  $C_{\text{emb}} > 0$ , such that for any  $f \in L^2([0, 1]^d)$ ,*

$$\|f\|_{\mathcal{B}_{2,1}^{-1}([0, 1]^d)} \leq C_{\text{emb}} \|f\|_{L_2([0, 1]^d)}.$$

**Lemma C.3** ([32, Lemma 29]). *Assume there exist  $\gamma, s > 0$  such that a density function  $q(x) \geq \gamma^{-1}$ ,  $\forall x \in [0, 1]^d$ , and such that  $q \in \mathcal{B}_{\infty, \infty}^s([0, 1]^d)$ . Let  $\tilde{q}_n$  be the wavelet projection based on an i.i.d. sample of size  $n$  drawn from the distribution with density  $q$ . Then, there exists  $c_b > 0$ , depending on  $[0, 1]^d$  and  $\|q\|_{\mathcal{B}_{\infty, \infty}^s([0, 1]^d)}$ , such that with probability at least  $1 - c_b/n^2$ ,*

$$\sup_{x \in [0, 1]^d} |q(x) - \tilde{q}_n(x)| \leq \gamma^{-1}/2.$$

**Proposition C.1** (Key estimation bound, Proposition 3.2). *Under Assumption 2.1-2.2,*

$$\mathbb{E} \left[ \int W_2^2(\hat{Q}_Y^z, Q_Y^z) \hat{R}(dz) \right] \leq C n^{-\frac{2s}{2s + d_Y + d_Z}},$$

where  $C = C_{\text{wb}}^2 \gamma^2 (16\gamma^5 (C_{\text{emb}} \gamma)^2 (C_{\text{emb}} + 1) C^\dagger + c_b)$ , and  $C^\dagger, c_b$  depend on  $d_Y, d_Z, q$ .

*Proof of Proposition C.1.* Denote the (wavelet) density of  $Q$  (resp.  $P$ ) by  $q$  (resp.  $p$ ), the (wavelet) density of  $\widehat{Q}$  (resp.  $\widehat{P}$ ) by  $\hat{q}$  (resp.  $\hat{p}$ ), and the (wavelet) density of  $\widehat{R}$  by  $\hat{r}$ . As for the wavelet projection, we replace  $\hat{p}$  with  $\tilde{p}$ . Then, by Assumption 2.1(i),

$$q(y|z) = \frac{q(y, z)}{q_Z(z)} = \frac{q(y, z)}{\int q(y, z) dy} \geq \gamma^{-2}.$$

Then, applying Lemma C.1, we get

$$\mathbb{E} \left[ \int W_2^2(\widehat{Q}_Y^z, Q_Y^z) \widehat{R}(dz) \right] \leq C_{\text{wb}}^2 \gamma^2 \mathbb{E} \left[ \int_{\mathcal{Z}} \|\hat{q}_Y^z(y) - q_Y^z(y)\|_{\mathcal{B}_{2,1}^{-1}([0,1]^{d_Y})}^2 d\widehat{R}(z) \right].$$

To further investigate the conditional densities, we apply Lemma C.3 under Assumption 2.2 and get, there exists  $c_b > 0$ , depending on  $d_Y, d_Z, q$ , such that with probability at least  $1 - c_b/n^2$ ,

$$\begin{aligned} \sup_{(y,z) \in [0,1]^{d_Y+d_Z}} |q(y, z) - \tilde{q}(y, z)| &\leq \gamma^{-1}/2, \\ \sup_{(y,z) \in [0,1]^{d_Y+d_Z}} |p(y, z) - \tilde{p}(y, z)| &\leq \gamma^{-1}/2. \end{aligned}$$

As a result,

$$\min_{(y,z) \in [0,1]^{d_Y+d_Z}} \tilde{q}(y, z) \geq \gamma^{-1}/2, \quad (11)$$

$$\tilde{r}(z) = \frac{1}{2}(\tilde{p}_Z(z) + \tilde{q}_Z(z)) \in [\gamma^{-1}/2, 2\gamma] \quad \forall z \in [0, 1]^{d_Z}. \quad (12)$$

Then, on this high probability event, the wavelet projection  $\tilde{q}$  is equal to the wavelet density estimator  $\hat{q}$  (so does  $\tilde{r}$ ), thus Eq. (11)-(12) also hold for  $\hat{q}, \hat{r}$ .

Also, on this high probability event, we apply the following decomposition to bound the right-hand side of the above inequality.

$$\begin{aligned} &\int_{[0,1]^{d_Z}} \|\hat{q}_Y^z(y) - q_Y^z(y)\|_{\mathcal{B}_{2,1}^{-1}([0,1]^{d_Y})}^2 d\widehat{R}(z) \\ &= \int_{[0,1]^{d_Z}} \left\| \frac{\hat{q}(\cdot, z)}{\hat{q}_Z(z)} - \frac{q(\cdot, z)}{q_Z(z)} \right\|_{\mathcal{B}_{2,1}^{-1}([0,1]^{d_Y})}^2 d\widehat{R}(z) \quad (\text{by the definition of } \hat{q}_Y^z(y)) \\ &\leq 2 \int_{[0,1]^{d_Z}} \frac{1}{\hat{q}_Z(z)^2} \|\hat{q}(\cdot, z) - q(\cdot, z)\|_{\mathcal{B}_{2,1}^{-1}([0,1]^{d_Y})}^2 + \|q(\cdot, z)\|_{\mathcal{B}_{2,1}^{-1}([0,1]^{d_Y})}^2 \left( \frac{1}{\hat{q}_Z(z)} - \frac{1}{q_Z(z)} \right)^2 d\widehat{R}(z) \\ &\leq 2(2\gamma)^3 \underbrace{\int_{[0,1]^{d_Z}} \|\hat{q}(\cdot, z) - q(\cdot, z)\|_{\mathcal{B}_{2,1}^{-1}([0,1]^{d_Y})}^2 dz}_{(\text{Term A})} + 2(2\gamma)^3 \gamma^2 (C_{\text{emb}} \gamma)^2 \underbrace{\int_{[0,1]^{d_Z}} (\hat{q}_Z(z) - q_Z(z))^2 dz}_{(\text{Term B})}, \end{aligned}$$

where the last inequality is due to Assumption 2.1 and Eq. (11)-(12). Specifically, by Lemma C.2,

$$\|q(\cdot, z)\|_{\mathcal{B}_{2,1}^{-1}([0,1]^{d_Y})}^2 \leq C_{\text{emb}}^2 \|q(\cdot, z)\|_{L^2([0,1]^{d_Y})}^2 \leq C_{\text{emb}}^2 \gamma^2 \quad \forall z \in [0, 1]^{d_Z}.$$

We analyze the two terms separately.

**(Term A).** By Lemma C.2,

$$\begin{aligned} &\int_{[0,1]^{d_Z}} \|\hat{q}(\cdot, z) - q(\cdot, z)\|_{\mathcal{B}_{2,1}^{-1}([0,1]^{d_Y})}^2 dz \\ &\leq C_{\text{emb}} \int_{[0,1]^{d_Z}} \|\hat{q}(\cdot, z) - q(\cdot, z)\|_{L^2([0,1]^{d_Y})}^2 dz \\ &\leq C_{\text{emb}} \|\hat{q} - q\|_{L^2([0,1]^{d_Y+d_Z})}^2. \end{aligned}$$

**(Term B).** Let  $\delta(y, z) = \hat{q}(y, z) - q(y, z)$ . Then, by the Cauchy–Schwarz inequality,

$$\begin{aligned} \int_{[0,1]^{d_Z}} (\hat{q}_Z(z) - q_Z(z))^2 dz &= \int_{[0,1]^{d_Z}} \left( \int_{[0,1]^{d_Y}} \delta(y, z) dy \right)^2 dz \\ &\leq \int_{[0,1]^{d_Z}} \left( \int_{[0,1]^{d_Y}} 1^2 dy \right) \left( \int_{[0,1]^{d_Y}} \delta(y, z)^2 dy \right) dz \\ &\leq \int_{[0,1]^{d_Y+d_Z}} (\hat{q}(y, z) - q(y, z))^2 dy dz, \\ &= \|\hat{q} - q\|_{L_2([0,1]^{d_Y+d_Z})}^2. \end{aligned}$$

Note that Eq. (11)-(12) implies  $\hat{q} = \tilde{q}$ , thus  $\hat{q}$  is the wavelet (linear) projection of the form

$$\hat{q} = \tilde{q} = \sum_{\zeta \in \Phi} \hat{\theta}_\zeta \zeta + \sum_{j=j_0}^{J_n} \sum_{\xi \in \Psi_j} \hat{\theta}_\xi \xi.$$

To bound  $\mathbb{E} \left[ \|\hat{q} - q\|_{L_2([0,1]^{d_Y+d_Z})}^2 \right]$ , we introduce the following result

**Proposition C.2.** *Under Assumption 2.1-2.2, there exists a constant  $C^\dagger$  depends on  $q, \gamma, s$  such that*

$$\mathbb{E} \left[ \int_{[0,1]^{d_Y+d_Z}} (\tilde{q}(y, z) - q(y, z))^2 dy dz \right] \leq C^\dagger n^{-\frac{2s}{2s+d_Y+d_Z}}.$$

Also note that [19] has a similar bound for the case  $d = 1$ .  
Combining the above results implies the desired result. □

## C.1 Proof of Proposition 3.1

*Proof of Proposition 3.1.* By [30, Proposition 2],

$$CW_h(P, Q) = \int W_h(P_Y^z, Q_Y^z) dP_Z(z).$$

Therefore, we have

$$\begin{aligned} & \left| CW_h(P, Q) - CW_h(\hat{P}, \hat{Q}) \right| \\ &= \left| \int W_h(P_Y^z, Q_Y^z) dP_Z(z) - \int W_h(\hat{P}_Y^z, \hat{Q}_Y^z) d\hat{P}_Z(z) \right| \\ &\leq \underbrace{\left| \int W_h(P_Y^z, Q_Y^z) dP_Z(z) - \int W_h(P_Y^z, \hat{Q}_Y^z) d\hat{P}_Z(z) \right|}_{\text{(Term A)}} + \underbrace{\left| \int W_h(P_Y^z, \hat{Q}_Y^z) d\hat{P}_Z(z) - \int W_h(\hat{P}_Y^z, \hat{Q}_Y^z) d\hat{P}_Z(z) \right|}_{\text{(Term B)}}. \end{aligned}$$

For **(Term A)**: we highlight that we consider the optimal coupling  $\pi_{Z, Z'} \in \mathcal{P}(\mathcal{Z}^2)$  that is attained in the

optimal transport  $W_1(P_Z, \widehat{P}_Z)$  to connect  $P_Z$  and  $\widehat{P}_Z$ , then

$$\begin{aligned}
(\text{Term A}) &= \left| \int W_h(P_Y^z, Q_Y^z) dP_Z(z) - \int W_h(P_Y^z, \widehat{Q}_Y^z) d\widehat{P}_Z(z) \right| \\
&= \left| \int W_h(P_Y^z, Q_Y^z) - W_h(P_Y^{z'}, \widehat{Q}_Y^{z'}) d\pi_{Z, Z'}(z, z') \right| \\
&\leq \int |W_h(P_Y^z, Q_Y^z) - W_h(P_Y^{z'}, \widehat{Q}_Y^{z'})| d\pi_{Z, Z'}(z, z') \\
&\leq L_h \int W_1(P_Y^z, P_Y^{z'}) + W_1(Q_Y^z, \widehat{Q}_Y^{z'}) d\pi_{Z, Z'}(z, z') \\
&\leq L_h \int L_p \|z - z'\|_2 + W_1(Q_Y^z, \widehat{Q}_Y^{z'}) d\pi_{Z, Z'}(z, z') \\
&\leq L_h \int 2L_p \|z - z'\|_2 + W_1(Q_Y^{z'}, \widehat{Q}_Y^{z'}) d\pi_{Z, Z'}(z, z') \\
&\leq 2L_h L_p W_1(P_Z, \widehat{P}_Z) + L_h \int W_1(Q_Y^{z'}, \widehat{Q}_Y^{z'}) d\widehat{P}_Z(z').
\end{aligned}$$

Here, the second inequality is due to [30, Lemma 5]; the third inequality is due to the condition; the last inequality is due to the definition of  $\pi$ , which achieves the *optimality* in  $W_1(P_Z, \widehat{P}_Z)$ .

For **(Term B)**: we have

$$\begin{aligned}
(\text{Term B}) &= \left| \int W_h(P_Y^z, \widehat{Q}_Y^z) d\widehat{P}_Z(z) - \int W_h(\widehat{P}_Y^z, \widehat{Q}_Y^z) d\widehat{P}_Z(z) \right| \\
&\leq \int |W_h(P_Y^z, \widehat{Q}_Y^z) - W_h(\widehat{P}_Y^z, \widehat{Q}_Y^z)| d\widehat{P}_Z(z) \\
&\leq L_h \int W_1(P_Y^z, \widehat{P}_Y^z) d\widehat{P}_Z(z),
\end{aligned}$$

where the last inequality is due to [30, Lemma 5].

Jointly, we get

$$|CW_h(\widehat{P}, \widehat{Q}) - CW_h(P, Q)| \leq 2L_h L_p W_1(P_Z, \widehat{P}_Z) + L_h \int W_1(P_Y^z, \widehat{P}_Y^z) + W_1(Q_Y^z, \widehat{Q}_Y^z) \widehat{P}_Z(dz).$$

□

## C.2 Proof of Theorem 3.1

*Proof of Theorem 3.1.* We first verify the conditions of Proposition 3.1 under Assumption 2.1 to 2.3.

- (i) Lipschitz continuity of  $h$  is assumed by Assumption 2.3.
- (ii) Under Assumption 2.1-2.2, by duality, we have

$$\begin{aligned}
W_1(Q_Y^z, Q_Y^{z'}) &\leq \int_{[0,1]^{d_Y}} |q(y|z) - q(y|z')| dy \\
&\leq \gamma \int_{[0,1]^{d_Y}} |q(y, z) - q(y, z')| dy \\
&\leq \gamma \max_{(y, z) \in [0,1]^{d_Y + d_Z}} \|\partial_z q(y, z)\|_2 \|z - z'\|_2.
\end{aligned}$$

Therefore, we set  $L_p = \gamma \max_{(y, z) \in [0,1]^{d_Y + d_Z}} \|\partial_z q(y, z)\|_2 \vee \|\partial_z p(y, z)\|_2$ .

Finally, apply Proposition 3.1, we have

$$\mathbb{E}[|V_c - \widehat{V}_{c,n}|] \leq 2L_h L_p \mathbb{E}[W_1(P_Z, \widehat{R}_n)] + L_h \mathbb{E} \left[ \int W_1(P_Y^z, \widehat{P}_{n,Y}^z) + W_1(Q_Y^z, \widehat{Q}_{n,Y}^z) \widehat{R}_n(dz) \right].$$

For the first term, applying Jensen's inequality, we get

$$\begin{aligned} & \mathbb{E}[W_1(P_Z, \widehat{R}_n)] \\ & \leq \frac{1}{2} (\mathbb{E}[W_1(P_Z, \widehat{P}_{n,Z})] + \mathbb{E}[W_1(P_Z, \widehat{Q}_{n,Z})]) \\ & \leq \frac{1}{2} \left( (\mathbb{E}[W_2^2(P_Z, \widehat{P}_{n,Z})])^{\frac{1}{2}} + (\mathbb{E}[W_2^2(P_Z, \widehat{Q}_{n,Z})])^{\frac{1}{2}} \right). \end{aligned}$$

Apply a similar reasoning as bounding the (Term B) in the proof of Proposition C.1: Under Assumption 2.1, applying Lemma C.1 - C.2, we get

$$\mathbb{E}[W_2^2(P_Z, \widehat{P}_{n,Z})] \leq C_{\text{wb}}^2 C_{\text{emb}}^2 \gamma \mathbb{E}[\|p - \hat{p}\|_2^2].$$

Then, applying Proposition C.2, we get

$$\mathbb{E}[W_2^2(P_Z, \widehat{P}_{n,Z})] \lesssim n^{-\frac{2s}{2s+d_Y+d_Z}}.$$

For the second term, applying Jensen's inequality and Proposition C.1, we get

$$\mathbb{E} \left[ \int W_1(Q_Y^z, \widehat{Q}_{n,Y}^z) \widehat{R}_n(dz) \right] \leq \left( \mathbb{E} \left[ \int W_2^2(Q_Y^z, \widehat{Q}_{n,Y}^z) \widehat{R}_n(dz) \right] \right)^{\frac{1}{2}} \lesssim n^{-\frac{s}{2s+d_Y+d_Z}}.$$

As a result, we get

$$\mathbb{E}[|V_c - \widehat{V}_{c,n}|] \leq CL_h n^{-\frac{s}{2s+d_Y+d_Z}},$$

where  $C$  is a constant that depends on  $P, Q, \gamma, s, d_Y, d_Z$ . □

### C.3 Proof of Proposition 3.3

The stability bound under quadratic objective stems from the case for unconditional Wasserstein-2 distance.

**Proposition C.3** (Proposition 12 in [32]). *Let  $P, Q \in \mathcal{P}_{\text{ac}}([0, 1]^d)$ . Assume that the Brenier potential  $\varphi_0$  between  $P, Q$  is a convex function such that  $\varphi_0 \in \mathcal{C}^2([0, 1]^d)$  and  $\varphi_0$  is  $\lambda$ -strongly convex, i.e., there exists  $\lambda > 0$  satisfying*

$$\frac{1}{\lambda} I_d \preceq \nabla^2 \varphi_0(x) \preceq \lambda I_d \quad \text{for all } x \in [0, 1]^d.$$

For any  $\widehat{P}, \widehat{Q} \in \mathcal{P}([0, 1]^d)$ ,

$$0 \leq W_2^2(\widehat{P}, \widehat{Q}) - W_2^2(P, Q) - \int \phi_0 d(\widehat{P} - P) - \int \psi_0 d(\widehat{Q} - Q) \leq \lambda (W_2(\widehat{P}, P) + W_2(\widehat{Q}, Q))^2, \quad (13)$$

where  $\phi_0(x) = \|x\|^2 - \varphi_0(x)$  and  $\psi_0(x) = \|x\|^2 - \varphi_0^*(x)$ , where  $\varphi_0^*$  is the convex conjugate of  $\varphi_0$ .

**Remark C.1.** We compare the conditional and the unconditional stability result. The upper bound in Proposition 3.3  $\int W_2^2(\widehat{P}_Y^z, P_Y^z) \widehat{R}(dz) + \int W_2^2(\widehat{Q}_Y^z, Q_Y^z) \widehat{R}(dz)$  is no smaller than  $W_2^2(\widehat{P}_Y^z \times \widehat{R}, P_Y^z \times \widehat{R}) + W_2^2(\widehat{Q}_Y^z \times \widehat{R}, Q_Y^z \times \widehat{R})$  by Lemma C.4, where the latter is similar to the upper bound  $W_2^2(\widehat{P}, P) + W_2^2(\widehat{Q}, Q)$  in Proposition C.3. A larger upper bound in Proposition 3.3 is consistent with the fact that COT is intrinsically more challenging than the unconditional counterpart.

**Lemma C.4** (Conditional Wasserstein distance V.S. Wasserstein distance). *Let  $P$  and  $Q$  be probability measures on  $\mathcal{Y} \times \mathcal{Z}$  with the same marginal distribution  $P_Z = Q_Z$  on  $\mathcal{Z}$ . For  $z \in \mathcal{Z}$ , let  $P_Y^z$  and  $Q_Y^z$  denote the corresponding conditional distributions on  $\mathcal{Y}$ . Consider the quadratic cost on  $\|y - y'\|^2$ . Then*

$$\mathbb{E}_{Z \sim P_Z} [W_2^2(P_Y^Z, Q_Y^Z)] \geq W_2^2(P, Q).$$

To obtain the strong convexity of the conditional potential functions in our setting, we shall leverage the following result.

**Lemma C.5** ([17, Corollary 3.2]). *Assume  $P, Q \in \mathcal{P}([0, 1]^d)$  with densities  $p, q$ . Assume the Brenier's potential  $\varphi_0$  between  $P, Q$  satisfies  $\varphi_0 \in C^2([0, 1]^d)$  and  $\gamma^{-1} \leq p(x), q(x) \leq \gamma \forall x \in [0, 1]^d$  for a constant  $\gamma > 0$ . Then there exists a constant  $\lambda > 0$ , depending only on  $\gamma$ , such that  $\varphi_0$  is  $\lambda$ -strongly convex.*

Now we are ready to prove the proposition.

*Proof of Proposition 3.3.* In the following, we denote  $\phi_z(y) := \phi(y, z)$ ,  $\psi_z(y) := \psi(y, z)$ .

First, applying Lemma C.5 under Assumption 2.1 ( $\gamma$ ) and also by the assumption that  $\|\phi(\cdot, z)\|_{C^2([0, 1]^{d_Y})}$  is bounded by  $C_2$  uniformly for  $z$ , we get, there exists a constant  $\lambda > 0$  that depends on  $\gamma$  and  $C_2$ , such that for any  $(y, z) \in [0, 1]^{d_Y + d_Z}$ ,

$$\lambda^{-1} I_{d_Y} \preceq \nabla_y^2 \varphi(y, z) \preceq \lambda I_{d_Y}.$$

For all  $z \in [0, 1]^{d_Z}$ , under Assumption 2.1 and with constant  $\lambda > 0$ , apply Proposition C.3 to  $(P_Y^z, Q_Y^z)$ , we get

$$\begin{aligned} 0 &\leq \underbrace{W_2(\widehat{P}_Y^z, \widehat{Q}_Y^z)^2 - W_2(P_Y^z, Q_Y^z)^2}_{:=\text{Term (a)}} - \underbrace{\int \phi_z d(\widehat{P}_Y^z - P_Y^z) - \int \psi_z d(\widehat{Q}_Y^z - Q_Y^z)}_{:=\text{Term (b)}} \\ &\leq \lambda \underbrace{\left( W_2(\widehat{P}_Y^z, P_Y^z) + W_2(\widehat{Q}_Y^z, Q_Y^z) \right)^2}_{:=\text{Term (c)}}, \end{aligned}$$

for any  $z \in [0, 1]^{d_Z}$ . To derive the final result, we integrate the term (a) to (c) in the inequality above with respect to the empirical marginal distribution  $\widehat{R}(dz) = \widehat{P}_Z(dz) = \widehat{Q}_Z(dz)$ . Here we use the alignment property that  $\widehat{P}$  and  $\widehat{Q}$  share the same marginal distribution of  $Z$ .

**Term (a).** By the alignment property of the estimated densities  $\widehat{R}(dz) = \widehat{P}_Z(dz) = \widehat{Q}_Z(dz)$ , we have

$$\int W_2(\widehat{P}_Y^z, \widehat{Q}_Y^z)^2 \widehat{R}(dz) = CW_2(\widehat{P}, \widehat{Q})^2.$$

In addition, by the alignment property of the true densities  $R(dz) = P_Z(dz) = Q_Z(dz)$ ,

$$\begin{aligned} \int W_2(P_Y^z, Q_Y^z)^2 \widehat{R}(dz) &= \int W_2(P_Y^z, Q_Y^z)^2 R(dz) + \int W_2(P_Y^z, Q_Y^z)^2 (\widehat{R}(dz) - R(dz)) \\ &= CW_2(P, Q)^2 + \int W_2(P_Y^z, Q_Y^z)^2 (\widehat{R}(dz) - R(dz)). \end{aligned} \tag{14}$$

**Term (b).** We have

$$\begin{aligned} &\int \int \phi_z(y) (\widehat{P}_Y^z(dy) - P_Y^z(dy)) \widehat{R}(dz) \\ &= \int \int \phi_z(y) (\widehat{P}_Y^z(dy) \widehat{R}(dz) - P_Y^z(dy) \widehat{R}(dz)) \\ &= \int \int \phi_z(y) (\widehat{P}_Y^z(dy) \widehat{R}(dz) - P_Y^z(dy) R(dz)) - \int \int \phi_z(y) P_Y^z(dy) (\widehat{R}(dz) - R(dz)) \\ &= \int \phi d(\widehat{P} - P) - \int \int \phi_z(y) P_Y^z(dy) (\widehat{R}(dz) - R(dz)), \end{aligned}$$

where we use the definition of  $\phi$  and  $\psi$ . Similarly,

$$\begin{aligned} &\int \int \psi_z(y) (\widehat{Q}_Y^z(dy) - Q_Y^z(dy)) \widehat{R}(dz) \\ &= \int \psi d(\widehat{Q} - Q) - \int \int \psi_z(y) Q_Y^z(dy) (\widehat{R}(dz) - R(dz)). \end{aligned}$$

By the optimality relation of COT,

$$W_2(P_Y^z, Q_Y^z)^2 = \int \phi_z(y) P_Y^z(dy) + \int \psi_z(y) Q_Y^z(dy).$$

Therefore, we have

$$\begin{aligned} & \int \int \phi_z(y) (\widehat{P}_Y^z(dy) - P_Y^z(dy)) \widehat{R}(dz) + \int \int \psi_z(y) (\widehat{Q}_Y^z(dy) - Q_Y^z(dy)) \widehat{R}(dz) \\ &= \int \phi d(\widehat{P} - P) + \int \psi d(\widehat{Q} - Q) - \int W_2(P_Y^z, Q_Y^z)^2 (\widehat{R}(dz) - R(dz)). \end{aligned} \quad (15)$$

**Term (c).** The integration of Term (c) over  $\widehat{R}(dz)$  together with the inequality  $(a+b)^2 < 2a^2 + 2b^2$  give the right hand side of the inequality of Proposition 3.3.

Note that the term  $\int \psi d(\widehat{Q} - Q) - \int W_2(P_Y^z, Q_Y^z)^2 (\widehat{R}(dz) - R(dz))$  shows up in both (14), (15) and are thus canceled. Combining term (a), term (b), and term (c), we get the desired result.  $\square$

## C.4 Proof of Theorem 3.2

First we need a lemma to prove the smoothness of  $\phi, \psi$ .

**Lemma C.6** (Smooth Kantorovich potential). *Under Assumption 2.1-2.2, when  $2s > d_Y + d_Z$ ,  $\varphi \in \mathcal{C}^{s+1}([0, 1]^{d_Y+d_Z})$ , then  $\phi, \psi \in \mathcal{C}^{s+1}([0, 1]^{d_Y+d_Z})$ .*

*Proof of Theorem 3.2.* Since  $s > d_Y + d_Z$ , thus  $s > 2$ . Since  $\varphi \in \mathcal{C}^{s+1}([0, 1]^{d_Y+d_Z})$ , we apply Proposition 3.3 and get

$$\begin{aligned} 0 &\leq CW_2(\widehat{P}_n^\dagger, \widehat{Q}_n^\dagger)^2 - CW_2(P, Q)^2 - \int \phi d(\widehat{P}_n^\dagger - P) - \int \psi d(\widehat{Q}_n^\dagger - Q) \\ &\leq 2\lambda \int W_2^2(\widehat{P}_Y^z, P_Y^z) + W_2^2(\widehat{Q}_Y^z, Q_Y^z) \widehat{R}_n(dz), \end{aligned}$$

where  $\lambda$  is a constant that depends on  $\gamma, \|\varphi\|_{\mathcal{C}^2}$ .

By Proposition C.1, we have

$$\mathbb{E} \left[ \int W_2^2(\widehat{P}_Y^z, P_Y^z) \widehat{R}(dz) \right] \vee \mathbb{E} \left[ \int W_2^2(\widehat{Q}_Y^z, Q_Y^z) \widehat{R}(dz) \right] \lesssim n^{-\frac{2s}{2s+d_Y+d_Z}}.$$

Therefore, when  $2s > d_Y + d_Z$ ,

$$\int W_2^2(\widehat{P}_Y^z, P_Y^z) + W_2^2(\widehat{Q}_Y^z, Q_Y^z) \widehat{R}_n(dz) = o_p(n^{-1/2}).$$

It remains to show that

$$\sqrt{n} \left( \int \phi d(\widehat{P}_n^\dagger - P) + \int \psi d(\widehat{Q}_n^\dagger - Q) \right) \xrightarrow{d} \mathcal{N}(0, \sigma^2).$$

We use  $\hat{r}(z)$  to denote the density of  $\widehat{R}_n(z)$ . We use  $\mathcal{Y} \times \mathcal{Z}$  and  $[0, 1]^{d_Y+d_Z}$  interchangeably. Since  $\mathcal{Y} \times \mathcal{Z}$  is compact and  $p(y, z), q(y, z), \phi(y, z), \psi(y, z) \in \mathcal{C}^{s+1}(\mathcal{Y} \times \mathcal{Z})$ , there exists  $M > 0$  such that  $p(y, z), q(y, z), |\phi(y, z)|, |\psi(y, z)| < M$  for any  $(y, z) \in \mathcal{Y} \times \mathcal{Z}$ .

According to Definition 3.1, we can decompose  $\int \phi d(\widehat{P}_n^\dagger - P)$  as

$$\int \phi d(\widehat{P}_n^\dagger - P) = \underbrace{\int \phi d(\widehat{P}_n^\dagger - \widehat{P}_n)}_{:=\text{Term (a)}} + \underbrace{\int \phi d(\widehat{P}_n - P)}_{:=\text{Term (b)}}.$$

**Term (a).** In the following, we ignore the dependence on  $n$ .

$$\begin{aligned}
\int \phi d(\widehat{P}_n^\dagger - \widehat{P}_n) &= \int \phi(y, z) \left( \frac{\widehat{p}(y, z)}{\widehat{p}_Z(z)} \widehat{r}(z) - \frac{\widehat{p}(y, z)}{\widehat{p}_Z(z)} \widehat{p}_Z(z) \right) dydz \quad (\text{Definition 3.1}) \\
&= \int \phi(y, z) \frac{\widehat{p}(y, z)}{\widehat{p}_Z(z)} (\widehat{r}(z) - \widehat{p}_Z(z)) dydz \\
&= \underbrace{\int \phi(y, z) \frac{p(y, z)}{p_Z(z)} (\widehat{r}(z) - \widehat{p}_Z(z)) dydz}_{:=\text{Term (a.1)}} \\
&\quad + \underbrace{\int \phi(y, z) \left( \frac{\widehat{p}(y, z)}{\widehat{p}_Z(z)} - \frac{p(y, z)}{p_Z(z)} \right) (\widehat{r}(z) - \widehat{p}_Z(z)) dydz}_{:=\text{Term (a.2)}}.
\end{aligned}$$

Term (a.1) is relatively straightforward as  $\widehat{r}(z)$  and  $\widehat{p}_Z(z)$  are based on marginalizing standard wavelet-based density estimators, and we postpone the analysis. For Term (a.2), by the Cauchy-Schwarz inequality,

$$\begin{aligned}
&\left( \int \phi(y, z) \left( \frac{\widehat{p}(y, z)}{\widehat{p}_Z(z)} - \frac{p(y, z)}{p_Z(z)} \right) (\widehat{r}(z) - \widehat{p}_Z(z)) dydz \right)^2 \\
&\leq M^2 \underbrace{\int \left( \frac{\widehat{p}(y, z)}{\widehat{p}_Z(z)} - \frac{p(y, z)}{p_Z(z)} \right)^2 dydz}_{:=\text{Term (a.2.1)}} \underbrace{\int (\widehat{r}(z) - \widehat{p}_Z(z))^2 dz}_{:=\text{Term (a.2.2)}}.
\end{aligned}$$

For Term (a.2.1), we decompose it as

$$\begin{aligned}
\text{Term (a.2.1)} &= \int \left( \frac{\widehat{p}(y, z)}{\widehat{p}_Z(z)} - \frac{p(y, z)}{\widehat{p}_Z(z)} + \frac{p(y, z)}{\widehat{p}_Z(z)} - \frac{p(y, z)}{p_Z(z)} \right)^2 dydz \\
&\leq 2 \int \frac{1}{\widehat{p}_Z(z)^2} (\widehat{p}(y, z) - p(y, z))^2 dydz + 2 \frac{M^2}{\widehat{p}_Z(z)^2 p_Z(z)^2} \int (\widehat{p}_Z(z) - p_Z(z))^2 dz.
\end{aligned} \tag{16}$$

Then, we apply the same reasoning as in the proof of Proposition C.1 that with probability at least  $1 - c/n^2$  for some constant  $c$ ,  $\widehat{p}_Z(z) \geq \gamma^{-1}/2 \forall z$ . Thus,

$$\text{Term (a.2.1)} \leq 2(2\gamma)^4 \int (\widehat{p}(y, z) - p(y, z))^2 dydz + 2M^2 \int (\widehat{p}_Z(z) - p_Z(z))^2 dz.$$

Again, by the same reasoning as in the proof of Proposition C.1, applying Proposition C.2, we get

$$\mathbb{E}[\text{Term (a.2.1)}] \lesssim n^{-\frac{2s}{2s+d_Y+d_Z}}.$$

When  $2s > d_Y + d_Z$ , Term (a.2.1) =  $o_p(n^{-1/2})$ .

For Term (a.2.2), since

$$\begin{aligned}
\widehat{r}(z) - \widehat{p}_Z(z) &= (\widehat{r}(z) - p_Z(z)) - (\widehat{p}_Z(z) - p_Z(z)), \\
&= \frac{1}{2}(\widehat{p}_Z(z) - p_Z(z)) + \frac{1}{2}(\widehat{q}_Z(z) - p_Z(z)) - (\widehat{p}_Z(z) - p_Z(z)) \quad (\text{Definition 3.1}).
\end{aligned}$$

Then, similarly, we have, when  $2s > d_Y + d_Z$ , Term (a.2.2) =  $o_p(n^{-1/2})$ .

Jointly, and we get Term (a.2) =  $o_p(n^{-1/2})$ , which implies that in Term (a.2) is ignorable.

Next, we bring Term (b), Term (a.1), as well as the counterparts for  $Q$  together. By the construction of  $\widehat{p}^\dagger(y, z)$  (Definition 3.1), we have  $\widehat{r}(z) = (\widehat{p}_Z(z) + \widehat{q}_Z(z))/2$ , which implies

$$-(\widehat{r}(z) - \widehat{p}_Z(z)) = \widehat{r}(z) - \widehat{q}_Z(z) = (\widehat{p}_Z(z) - \widehat{q}_Z(z))/2. \tag{17}$$

Then

$$\begin{aligned}
& \int \phi d(\widehat{P}_n^\dagger - P) + \int \psi d(\widehat{Q}_n^\dagger - Q) \\
&= \underbrace{\int \phi(y, z) \frac{p(y, z)}{p_Z(z)} (\widehat{r}(z) - \widehat{p}_Z(z)) dy dz}_{\text{Term (a.1)}} + \underbrace{\int \phi(y, z) (\widehat{p}(y, z) - p(y, z)) dy dz}_{\text{Term (b)}} \\
&+ \int \psi(y, z) \frac{q(y, z)}{q_Z(z)} (\widehat{r}(z) - \widehat{q}_Z(z)) dy dz + \int \psi(y, z) (\widehat{q}(y, z) - q(y, z)) dy dz + o_p(n^{-1/2}) \\
&= \int \left( \phi(y, z) \frac{p(y, z)}{p_Z(z)} - \psi(y, z) \frac{q(y, z)}{q_Z(z)} \right) \left( \frac{\widehat{q}_Z(z) - \widehat{p}_Z(z)}{2} \right) dy dz \quad (\text{by Eq. (17)}) \\
&+ \int \phi(y, z) (\widehat{p}(y, z) - p(y, z)) dy dz + \int \psi(y, z) (\widehat{q}(y, z) - q(y, z)) dy dz + o_p(n^{-1/2}) \\
&= \underbrace{\int - \left( \phi(y, z) \frac{p(y, z)}{p_Z(z)} - \psi(y, z) \frac{q(y, z)}{q_Z(z)} \right) \left( \frac{\widehat{p}_Z(z) - p_Z(z)}{2} \right) + \phi(y, z) (\widehat{p}(y, z) - p(y, z)) dy dz}_{:=\text{Term (c)}} \\
&+ \underbrace{\int \left( \phi(y, z) \frac{p(y, z)}{p_Z(z)} - \psi(y, z) \frac{q(y, z)}{q_Z(z)} \right) \left( \frac{\widehat{q}_Z(z) - q_Z(z)}{2} \right) + \psi(y, z) (\widehat{q}(y, z) - q(y, z)) dy dz}_{:=\text{Term (d)}} + o_p(n^{-1/2}) \\
&\quad (p_Z(z) = q_Z(z) \text{ and } \widehat{q}_Z(z) - \widehat{p}_Z(z) = \widehat{q}_Z(z) - q_Z(z) - (\widehat{p}_Z(z) - p_Z(z)))
\end{aligned}$$

For Term (c), as  $\widehat{p}_Z(z) - p_Z(z) = \int \widehat{p}(y, z) - p(y, z) dy dz$ ,

$$\begin{aligned}
\text{term (c)} &= \int \left( \int - \left( \phi(y', z) \frac{p(y', z)}{p_Z(z)} - \psi(y', z) \frac{q(y', z)}{q_Z(z)} \right) dy' \right) \left( \int \left( \frac{\widehat{p}(y, z) - p(y, z)}{2} \right) dy \right) dz \\
&+ \int \phi(y, z) (\widehat{p}(y, z) - p(y, z)) dy dz \\
&= \int \underbrace{\left( \phi(y, z) - \frac{1}{2} \left( \int \left( \phi(y', z) \frac{p(y', z)}{p_Z(z)} - \psi(y', z) \frac{q(y', z)}{q_Z(z)} \right) dy' \right) \right)}_{=\eta(y, z)} (\widehat{p}(y, z) - p(y, z)) dy dz.
\end{aligned}$$

As  $\phi(y, z), \psi(y, z), p(y, z), q(y, z) \in \mathcal{C}^{s+1}(\mathcal{Y} \times \mathcal{Z})$  and  $p_Z, q_Z \geq \gamma^{-1}$ , we have  $\eta(y, z) \in \mathcal{C}^{s+1}(\mathcal{Y} \times \mathcal{Z})$ . By Lemma 11 (control bias) and Lemma 66 (central limit theorem) of [32], we establish the central limit theorem for  $\sqrt{n} \times$  term (c) with the variance

$$2\text{Var}_P(\eta(y, z)) = 2\text{Var}_P \left( \phi(Y, Z) - \frac{\mathbb{E}_P[\phi(Y, Z) | Z] - \mathbb{E}_Q[\psi(Y, Z) | Z]}{2} \right).$$

The same argument applies to term (d). Note that term (c) and term (d) are based on different observations and thus independent, which yields a central limit theorem for their sum scaled by  $\sqrt{n}$  with the asymptotic variance  $2(\text{Var}_P(\eta(y, z)) + \text{Var}_Q(\kappa(y, z)))$ .  $\square$

## C.5 Proof of Proposition 2.2

*Proof of Proposition 2.2.* The first part  $\mathcal{C}^s([0, 1]^d) \subseteq \mathcal{B}_{\infty, \infty}^s([0, 1]^d)$  has been proved in [32, Lemma 25]. We focus on the second part:  $\mathcal{C}^s \subseteq \mathcal{B}_{2, 2}^{s-\varepsilon}$  for any  $\varepsilon > 0$ .

**Lemma C.7** (Hölder to Sobolev/Besov with  $\varepsilon$ -loss). *Let  $d, s > 0$ . For any  $\varepsilon > 0$ , there exists a constant  $C = C(d, s, \varepsilon)$  such that*

$$\|f\|_{\mathcal{B}_{2, 2}^{s-\varepsilon}([0, 1]^d)} \leq C \|f\|_{\mathcal{C}^s([0, 1]^d)} \quad \forall f \in \mathcal{C}^s([0, 1]^d).$$

*Equivalently,  $\mathcal{C}^s([0, 1]^d) \hookrightarrow \mathcal{B}_{2, 2}^{s-\varepsilon}([0, 1]^d)$ .*

*Proof.* Fix  $\varepsilon > 0$  and set  $t = s - \varepsilon$ . Let  $\{\phi_k\}_{k \in \mathcal{I}_0}$  be the (boundary-corrected) scaling functions at the coarsest resolution and  $\{\psi_{j,k}\}_{j \geq j_0, k \in \mathcal{I}_j}$  be a compactly supported, boundary-corrected wavelet basis on  $[0, 1]^d$  with regularity strictly larger than  $s$ . Then every  $f \in L^2([0, 1]^d)$  admits the wavelet expansion

$$f = \sum_{k \in \mathcal{I}_0} \alpha_k \phi_k + \sum_{j \geq j_0} \sum_{k \in \mathcal{I}_j} \beta_{j,k} \psi_{j,k}, \quad \alpha_k = \langle f, \phi_k \rangle, \quad \beta_{j,k} = \langle f, \psi_{j,k} \rangle.$$

We use the standard wavelet characterizations of Besov norms on  $[0, 1]^d$  (with boundary correction):

$$\|f\|_{B_{2,2}^s([0,1]^d)}^2 \lesssim \sum_{k \in \mathcal{I}_0} |\alpha_k|^2 + \sum_{j \geq j_0} 2^{2jt} \sum_{k \in \mathcal{I}_j} |\beta_{j,k}|^2. \quad (18)$$

Let  $M := \|f\|_{C^s([0,1]^d)}$ . By the proof of [32, Lemma 25], we have

$$\sup_{k \in \mathcal{I}_j} |\beta_{j,k}| \leq C_1 M 2^{-j(s+d/2)} \quad \forall j \geq j_0, \quad (19)$$

for some constant  $C_1$  depending only on  $(d, s)$  and the chosen wavelet system.

Next, recall that the number of wavelets at level  $j$  satisfies  $|\mathcal{I}_j| \lesssim 2^{jd}$ . Using (19),

$$\sum_{k \in \mathcal{I}_j} |\beta_{j,k}|^2 \leq |\mathcal{I}_j| \left( \sup_{k \in \mathcal{I}_j} |\beta_{j,k}| \right)^2 \lesssim 2^{jd} \cdot (M^2 2^{-2j(s+d/2)}) = C_2 M^2 2^{-2js}, \quad (20)$$

for some constant  $C_2$ .

Multiplying (20) by  $2^{2jt} = 2^{2j(s-\varepsilon)}$  yields

$$2^{2jt} \sum_{k \in \mathcal{I}_j} |\beta_{j,k}|^2 \leq C_2 M^2 2^{2j(s-\varepsilon)} \cdot 2^{-2js} = C_2 M^2 2^{-2j\varepsilon}.$$

Summing over  $j \geq j_0$  and using  $\sum_{j \geq j_0} 2^{-2j\varepsilon} < \infty$ , we obtain

$$\sum_{j \geq j_0} 2^{2jt} \sum_{k \in \mathcal{I}_j} |\beta_{j,k}|^2 \leq C_3 M^2, \quad (21)$$

for a constant  $C_3 = C_3(d, s, \varepsilon)$ .

Finally, again by [32, Lemma 2],  $\sup_{k \in \mathcal{I}_0} |\alpha_k| \leq M$ , thus

$$\sum_{k \in \mathcal{I}_0} |\alpha_k|^2 \leq |\mathcal{I}_0| \left( \sup_{k \in \mathcal{I}_0} |\alpha_k| \right)^2 \leq C_4 M^2. \quad (22)$$

Combining (18)–(22) gives

$$\|f\|_{B_{2,2}^s([0,1]^d)}^2 \leq C_5 M^2,$$

hence  $\|f\|_{B_{2,2}^{s-\varepsilon}([0,1]^d)} \leq \sqrt{C_5} \|f\|_{C^s([0,1]^d)}$ , proving the claim.  $\square$

$\square$

## C.6 Proof of Proposition C.2

In this section, we prove Proposition C.2 in a more general way (see Theorem C.1). By Assumption 2.2 and Proposition 2.2,  $p, q \in \mathcal{B}_{2,2}^s([0, 1]^{d_Y+d_Z})$  and  $\gamma^{-1} \leq p, q \leq \gamma$ , thus satisfying Assumptions C.1–C.2.

**Assumption C.1** (Smoothness and boundedness). *Let  $p$  be a density on  $[0, 1]^d$  such that  $p \in \mathcal{B}_{2,2}^s([0, 1]^d)$  for some  $s > 0$ . Assume also  $0 \leq p \leq M$  a.e. for some  $M < \infty$ .*

**Assumption C.2** (Wavelet basis on  $[0, 1]^d$ ). *Let  $\{\phi_{j_0,k}^{\text{bc}}\}_{k \in \mathcal{K}_0(j_0)} \cup \{\psi_{j,k,\ell}^{\text{bc}}\}_{j \geq j_0, k \in \mathcal{K}_0(j), \ell \in \{0,1\}^d \setminus \{0\}}$  be an orthonormal (boundary-corrected) wavelet basis of  $L^2([0, 1]^d)$ . Write the coefficients of  $p$  as*

$$\alpha_k := \langle p, \phi_{j_0,k}^{\text{bc}} \rangle, \quad \beta_{j,k,\ell} := \langle p, \psi_{j,k,\ell}^{\text{bc}} \rangle.$$

**(Linear projection estimator).** Let  $X_1, \dots, X_n \sim p$  i.i.d. Fix an integer  $J \geq j_0$  and define the empirical coefficients

$$\hat{\alpha}_k := \frac{1}{n} \sum_{i=1}^n \phi_{j_0, k}^{\text{bc}}(X_i), \quad \hat{\beta}_{j, k, \ell} := \frac{1}{n} \sum_{i=1}^n \psi_{j, k, \ell}^{\text{bc}}(X_i), \quad j_0 \leq j \leq J.$$

Define the (untruncated) projection estimator

$$\tilde{p}_J(x) := \sum_{k \in \mathcal{K}(j_0)} \hat{\alpha}_k \phi_{j_0, k}^{\text{bc}}(x) + \sum_{j=j_0}^J \sum_{\ell \neq 0} \sum_{k \in \mathcal{K}(j)} \hat{\beta}_{j, k, \ell} \psi_{j, k, \ell}^{\text{bc}}(x).$$

Define the truncated (clipped) estimator

$$\tilde{p}_J^\dagger(x) := (\tilde{p}_J(x))_{[0, M]} := \min\{M, \max\{0, \tilde{p}_J(x)\}\}.$$

**Theorem C.1** ( $L^2$  risk of the truncated projection estimator). *Under Assumptions C.1–C.2,*

$$\mathbb{E} \|\tilde{p}_J^\dagger - p\|_{L^2([0, 1]^d)}^2 \lesssim 2^{-2Js} + \frac{2^{Jd}}{n}.$$

Consequently, choosing  $2^J \asymp n^{1/(2s+d)}$  yields

$$\mathbb{E} \|\tilde{p}_J^\dagger - p\|_2^2 \lesssim n^{-\frac{2s}{2s+d}},$$

and moreover the risk is always bounded by  $\lesssim n^{-1}$ , hence

$$\mathbb{E} \|\tilde{p}_J^\dagger - p\|_2^2 \lesssim n^{-\frac{2s}{2s+d}}.$$

The hidden constants depend only on  $(s, d)$ , the wavelet family, and  $M$ .

*Proof.* **Step 0 (Truncation cannot increase  $L^2$  error).** The clipping map  $T(u) = (u)_{[0, M]}$  is 1-Lipschitz on  $\mathbb{R}$ , i.e.  $|T(u) - T(v)| \leq |u - v|$ . Therefore,

$$\|\tilde{p}_J^\dagger - p\|_2^2 = \|T(\tilde{p}_J) - T(p)\|_2^2 \leq \|\tilde{p}_J - p\|_2^2,$$

since  $p \in [0, M]$  a.e. by assumption. Hence it suffices to bound  $\mathbb{E} \|\tilde{p}_J - p\|_2^2$ .

**Step 1 (Orthogonal bias–variance decomposition).** By orthonormality,

$$\|\tilde{p}_J - p\|_2^2 = \|\tilde{p}_J - p_J\|_2^2 + \|p_J - p\|_2^2,$$

and taking expectations gives

$$\mathbb{E} \|\tilde{p}_J - p\|_2^2 = \mathbb{E} \|\tilde{p}_J - p_J\|_2^2 + \|p_J - p\|_2^2.$$

**Step 2 (Bias bound).** Since  $p \in B_{2,2}^s([0, 1]^d)$ , the wavelet characterization yields the tail energy bound

$$\|p - p_J\|_2^2 = \sum_{j>J} \sum_{\ell \neq 0} \sum_{k \in \mathcal{K}(j)} \beta_{j, k, \ell}^2 \lesssim 2^{-2Js} \|p\|_{B_{2,2}^s}^2.$$

**Step 3 (Variance bound).** By orthonormality,

$$\mathbb{E} \|\tilde{p}_J - p_J\|_2^2 = \sum_{k \in \mathcal{K}(j_0)} \mathbb{E}(\hat{\alpha}_k - \alpha_k)^2 + \sum_{j=j_0}^J \sum_{\ell \neq 0} \sum_{k \in \mathcal{K}(j)} \mathbb{E}(\hat{\beta}_{j, k, \ell} - \beta_{j, k, \ell})^2.$$

Each empirical coefficient is an average of i.i.d. terms, so

$$\mathbb{E}(\hat{\beta}_{j, k, \ell} - \beta_{j, k, \ell})^2 = \frac{1}{n} \text{Var}(\psi_{j, k, \ell}^{\text{bc}}(X_1)) \leq \frac{1}{n} \mathbb{E}[\psi_{j, k, \ell}^{\text{bc}}(X_1)^2] \leq \frac{\|p\|_\infty}{n} \int_{[0, 1]^d} (\psi_{j, k, \ell}^{\text{bc}}(x))^2 dx = \frac{\|p\|_\infty}{n},$$

using  $\|p\|_\infty \leq M$  and  $\|\psi_{j,k,\ell}^{\text{bc}}\|_2 = 1$ . The same bound holds for the scaling coefficients. Hence

$$\mathbb{E}\|\tilde{p}_J - p_J\|_2^2 \lesssim \frac{1}{n} \left( |\mathcal{K}(j_0)| + \sum_{j=j_0}^J \sum_{\ell \neq 0} |\mathcal{K}_0(j)| \right).$$

On  $[0, 1]^d$ ,  $|\mathcal{K}(j)| \asymp 2^{jd}$  and there are  $(2^d - 1)$  wavelet types  $\ell \neq 0$ , so

$$\mathbb{E}\|\tilde{p}_J - p_J\|_2^2 \lesssim \frac{1}{n} \sum_{j=j_0}^J 2^{jd} \lesssim \frac{2^{Jd}}{n}.$$

**Step 4 (Combine and optimize).** Combining Steps 2–3 gives

$$\mathbb{E}\|\tilde{p}_J - p\|_2^2 \lesssim 2^{-2Js} + \frac{2^{Jd}}{n}.$$

Since  $\mathbb{E}\|\tilde{p}_J^\dagger - p\|_2^2 \leq \mathbb{E}\|\tilde{p}_J - p\|_2^2$ , the same bound holds for  $\tilde{p}_J^\dagger$ . Choosing  $2^J \asymp n^{1/(2s+d)}$  balances the two terms and yields  $\mathbb{E}\|\tilde{p}_J^\dagger - p\|_2^2 \lesssim n^{-2s/(2s+d)}$ .  $\square$

## C.7 Proof of Lemmas

### C.7.1 Proof of Lemma C.1

*Proof of Lemma C.1.* Plug  $p = 1/2$  in Theorem 4 in [37] and we finish the proof.  $\square$

### C.7.2 Proof of Lemma C.2

*Proof of Lemma C.2.* Let  $\{\psi_\lambda\}_{\lambda \in \Lambda}$  be an orthonormal wavelet basis of  $L^2([0, 1]^d)$ , and let  $\Lambda = \bigsqcup_{j \geq j_0} \Lambda_j$  denote the decomposition of indices by scale. Fix  $f \in L^2([0, 1]^d)$ , write its wavelet expansion

$$f = f_{<j_0} + \sum_{j \geq j_0} f_j, \quad f_j = \sum_{\lambda \in \Lambda_j} \alpha(\lambda) \psi_\lambda,$$

where  $f_{<j_0}$  is the coarse (scaling) component.

For each  $j \geq j_0$ , since  $\{\psi_\lambda\}_{\lambda \in \Lambda_j}$  is an orthonormal basis at level  $j$ , Parseval's identity then gives

$$\|f_j\|_{L^2([0,1]^d)}^2 = \sum_{\lambda \in \Lambda_j} |\alpha(\lambda)|^2, \quad \text{hence} \quad \|f_j\|_{L^2([0,1]^d)} = \left( \sum_{\lambda \in \Lambda_j} |\alpha(\lambda)|^2 \right)^{1/2}. \quad (23)$$

Therefore the left-hand side can be rewritten as

$$\left( \sum_{j \geq j_0} 2^{-j} \left( \sum_{\lambda \in \Lambda_j} |\alpha(\lambda)|^2 \right)^{1/2} \right)^2 = \left( \sum_{j \geq j_0} 2^{-j} \|f_j\|_{L^2([0,1]^d)} \right)^2.$$

Apply the Cauchy–Schwarz inequality to the sequences  $a_j = 2^{-j}$  and  $b_j = \|f_j\|_{L^2([0,1]^d)}$ :

$$\sum_{j \geq j_0} 2^{-j} \|f_j\|_{L^2([0,1]^d)} \leq \left( \sum_{j \geq j_0} 2^{-2j} \right)^{1/2} \left( \sum_{j \geq j_0} \|f_j\|_{L^2([0,1]^d)}^2 \right)^{1/2}. \quad (24)$$

Squaring (24) yields

$$\left( \sum_{j \geq j_0} 2^{-j} \|f_j\|_{L^2([0,1]^d)} \right)^2 \leq \left( \sum_{j \geq j_0} 2^{-2j} \right) \left( \sum_{j \geq j_0} \|f_j\|_{L^2([0,1]^d)}^2 \right). \quad (25)$$

Next, by the orthogonal decomposition

$$\|f\|_{L^2([0,1]^d)} = (\|f_{<j_0}\|_{L^2([0,1]^d)}^2 + \sum_{j \geq j_0} \|f_j\|_{L^2([0,1]^d)}^2)^{\frac{1}{2}} \geq \frac{1}{2} \left( \|f_{<j_0}\|_{L^2([0,1]^d)} + \left( \sum_{j \geq j_0} \|f_j\|_{L^2([0,1]^d)}^2 \right)^{\frac{1}{2}} \right).$$

Substituting this bound into (25) gives

$$\left( \sum_{j \geq j_0} 2^{-2j} \right)^{\frac{1}{2}} \|f_{<j_0}\|_{L^2([0,1]^d)} + \sum_{j \geq j_0} 2^{-j} \|f_j\|_{L^2([0,1]^d)} \leq 2 \left( \sum_{j \geq j_0} 2^{-2j} \right)^{\frac{1}{2}} \|f\|_{L^2([0,1]^d)}.$$

Finally, combining this with

$$\|f\|_{\mathcal{B}_{2,1}^{-1}([0,1]^d)} = \|f_{<j_0}\|_{L^2([0,1]^d)} + \sum_{j \geq j_0} 2^{-j} \|f_j\|_{L^2([0,1]^d)}$$

concludes the proof.  $\square$

### C.7.3 Proof of Lemma C.4

*Proof of Lemma C.4.* For each  $z \in \mathcal{Z}$ , let  $\pi_Z^*$  be an optimal coupling between  $P_Y^z$  and  $Q_Y^z$  for the cost  $\|y - y'\|^2$ . Define a coupling  $\pi^*$  on  $(\mathcal{Y} \times \mathcal{Z})^2$  via

$$\pi^*(dy, dz, dy', dz') := P_Z(dz) \pi_Z^*(dy, dy') \delta_Z(dz').$$

By construction, the first marginal of  $\pi^*$  is  $P$  and the second marginal is  $Q$ , hence  $\pi^* \in \Pi(P, Q)$ . Under the cost  $c((y, z), (y', z')) = \|y - y'\|^2$ , the transport cost of  $\pi$  is

$$\int \|y - y'\|^2 d\pi^* = \int \left( \int \|y - y'\|^2 d\pi_Z^*(y, y') \right) P_Z(dz) = \mathbb{E}_{Z \sim P_Z} [W_2^2(P(Y | Z), Q(Y | Z))].$$

Since  $W_2^2(P, Q)$  is the infimum of  $\int \|y - y'\|^2 d\pi$  over all  $\pi \in \Pi(P, Q)$ , we conclude that

$$W_2^2(P, Q) \leq \int \|y - y'\|^2 d\pi^* = \mathbb{E}_{Z \sim P_Z} [W_2^2(P(Y | Z), Q(Y | Z))].$$

$\square$

### C.7.4 Proof of Lemma C.6

*Proof of Lemma C.6.* Since  $\phi(y, z) = \|y\|_2^2 - \varphi(y, z)$ , then  $\phi \in \mathcal{C}^{s+1}([0, 1]^{d_Y + d_Z})$ .

As for  $\psi$ , note that  $\psi(y, z) = \|y\|_2^2 - \varphi^*(y, z)$ , and

$$\nabla_y^2 \varphi^*(y, z) = \nabla_y^2 \varphi(\nabla_y \varphi^*(y, z), z)^{-1} \quad (\star)$$

where the convex conjugate is defined with respect to  $y$ , i.e.,  $\varphi^*(y, z) := \sup_{y' \in [0, 1]^{d_Y}} \{y'^T y' - \varphi(y', z)\}$ .

By Lemma C.5, there is a constant  $\lambda > 0$ , such that

$$\frac{1}{\lambda} I_{d_Y} \preceq \nabla_y^2 \varphi(y, z) \preceq \lambda I_{d_Y} \quad \forall y, z \in [0, 1]^{d_Y + d_Z}.$$

Therefore, by  $(\star)$  and  $\varphi \in \mathcal{C}^{s+1}([0, 1]^{d_Y + d_Z})$ , we get  $\varphi^* \in \mathcal{C}^{s+1}([0, 1]^{d_Y + d_Z})$ , so does  $\psi$ .  $\square$

## D Algorithms

### D.1 Wavelet-based Density Estimation

We provide a detailed Algorithm 1 for the wavelet-based density estimation described in Definition 2.3.

---

**Algorithm 1:** Boundary-corrected wavelet density estimator for the joint density of  $(Y, Z)$ 


---

**Input:** Samples  $(Y_i, Z_i) \in [0, 1]^{d_Y + d_Z}$  for  $i = 1, \dots, n$ ; wavelet family with smoothness  $s$ ; coarse level  $J_0 \geq \lceil \log_2(s/0.18 + 1) \rceil + 1$ .

**Output:** Estimated joint density  $\widehat{f}_{Y,Z}$  on  $[0, 1]^{d_Y + d_Z}$ .

**Notation.** Let  $d := d_Y + d_Z$  and  $X_i := (Y_i, Z_i) \in [0, 1]^d$ . Let  $\{\phi_{J_0,k}^{\text{bc}}\}_{k \in \mathcal{K}_{J_0}}$  be the *boundary-corrected* scaling functions at level  $J_0$ , and for each  $j \geq J_0$  let  $\{\psi_{j,k,\ell}^{\text{bc}}\}_{k \in \mathcal{K}_j, \ell \in \mathcal{L}}$  be the boundary-corrected wavelets (where  $\ell$  indexes the  $2^d - 1$  multivariate wavelet types in  $d$  dimensions). Basis functions are supported on  $[0, 1]^d$  and form an orthonormal basis of  $L^2([0, 1]^d)$ .

**Step 1: Choose resolution levels.**

Pick  $(J_0, J)$  such that  $J_0$  fixed small,  $J \geq J_0$ , and  $J \asymp \frac{\log_2(n)}{2s + d_Y + d_Z}$ .

**Step 2: Compute empirical wavelet coefficients.**

```

foreach  $k \in \mathcal{K}_{J_0}$  do
  |  $\widehat{\alpha}_{J_0,k} \leftarrow \frac{1}{n} \sum_{i=1}^n \phi_{J_0,k}^{\text{bc}}(X_i)$ ;
end
for  $j = J_0$  to  $J$  do
  | foreach  $\ell \in \mathcal{L}$  do
    | foreach  $k \in \mathcal{K}_j$  do
      | |  $\widehat{\beta}_{j,k,\ell} \leftarrow \frac{1}{n} \sum_{i=1}^n \psi_{j,k,\ell}^{\text{bc}}(X_i)$ ;
      | end
    | end
  | end
end

```

**Step 3 (optional): Threshold / shrink detail coefficients.**

```

for  $j = J_0$  to  $J$  do
  | foreach  $\ell \in \mathcal{L}$  do
    | foreach  $k \in \mathcal{K}_j$  do
      | |  $\widetilde{\beta}_{j,k,\ell} \leftarrow \mathcal{T}(\widehat{\beta}_{j,k,\ell}; \lambda_j)$ ;
      | end
    | end
  | end
end
if no thresholding then
  |  $\widetilde{\beta}_{j,k,\ell} \leftarrow \widehat{\beta}_{j,k,\ell}$  for all  $(j, k, \ell)$ ;
end

```

**Step 4: Assemble the estimator.**

Define, for any  $x \in [0, 1]^d$ ,

$$\widehat{f}_{Y,Z}(x) := \sum_{k \in \mathcal{K}_{J_0}} \widehat{\alpha}_{J_0,k} \phi_{J_0,k}^{\text{bc}}(x) + \sum_{j=J_0}^J \sum_{\ell \in \mathcal{L}} \sum_{k \in \mathcal{K}_j} \widetilde{\beta}_{j,k,\ell} \psi_{j,k,\ell}^{\text{bc}}(x).$$

**Step 5: Enforce density constraints.**

```

if nonnegativity flag then
  |  $\widehat{f}_{Y,Z}(x) \leftarrow \max\{\widehat{f}_{Y,Z}(x), 0\}$ ;
end
if normalization flag then
  |  $c \leftarrow \int_{[0,1]^d} \widehat{f}_{Y,Z}(x) dx$ ;
  |  $\widehat{f}_{Y,Z}(x) \leftarrow \widehat{f}_{Y,Z}(x)/c$ ;
end
return  $\widehat{f}_{Y,Z}$ ;

```

---

## D.2 Optimal Transport Problem with Estimated Densities

Given the estimated joint densities  $\widehat{Q}$  and  $\widehat{P}$  of  $(Y_i(0), Z_i)$  and  $(Y_i(1), Z_i)$  together with the estimated marginal density of  $Z_i$ , we generate synthetic observations via a two-step hierarchical procedure.

1. We first draw  $N_1$  covariates  $Z$  from its marginal distribution.
2. Conditional on each sampled  $Z$ , draw outcomes from the corresponding conditional distributions  $\widehat{P}(Y(1) | Z)$ ,  $\widehat{Q}(Y(1) | Z)$  to get  $N_2$  observations for each group.

For estimation, we first for each  $Z$  solve an optimal transport problem. We then average over  $Z$  to get the final estimation.

Given the estimated joint densities  $\widehat{P}$  and  $\widehat{Q}$  of  $(Y_i(1), Z_i)$  and  $(Y_i(0), Z_i)$ , together with an estimate of the marginal density of  $Z$ , we generate synthetic data through a hierarchical sampling scheme designed to mimic the joint structure of the population.

1. Draw  $N_1$  samples of  $Z$  from its estimated marginal distribution.
2. Conditional on each sampled value of  $Z$ , draw  $N_2$  outcomes from the conditional densities  $\widehat{P}(Y(1) | Z)$  and  $\widehat{Q}(Y(0) | Z)$ .

We emphasize that these generated samples are not the original observations, but are Monte Carlo draws from the estimated density. To estimate the optimal objective value, we solve an optimal transport problem separately at each sampled  $Z$ , and average the resulting objective values over the sampled covariates to obtain the final estimate. Details are summarized in Algorithm 2.

There are a variety of approaches for sampling from an estimated density [39], including rejection sampling, importance sampling, Markov chain Monte Carlo (MCMC) methods such as Metropolis–Hastings and Gibbs sampling. Algorithm 2, we adopt a discretization-based sampler for its favorable practical stability. Specifically, we first discretize the support of the estimated density into a fine grid. The estimated density is then evaluated on this grid and normalized to form a discrete probability distribution. Samples are subsequently drawn from this grid according to the discrete probabilities. We remark that this discretization step differs from that used by [30], where the discretization is used as part of the estimation procedure and applied to the observed dataset. In contrast, here the discretization is used as a post-estimation device for sampling from the already constructed continuous density estimate. As a result, it does not affect the statistical properties of the estimator, but only serves as a practical mechanism for Monte Carlo approximation of the Wasserstein distance.

## E Additional Numerical Experiment

### E.1 Simulation Details of Estimation

#### E.1.1 Wavelet Algorithm Parameters

- `wavelet = "db4"`: Daubechies-4 wavelet basis, chosen for compact support and good smoothness properties.
- `mode = "periodization"`: boundary handling rule that treats the support as periodic, avoiding boundary artifacts for data supported on  $[0, 1]^d$ .
- `J_joint = 4`: wavelet resolution level for estimating the joint density  $\widehat{p}_{Y,Z}(y, z)$ . Larger values lead to finer resolution (lower bias, higher variance) and constitute the primary smoothing parameter.
- `J_z = 6`: wavelet resolution level for estimating the marginal density  $\widehat{p}_Z(z)$ . A higher level is used since  $Z$  is lower dimensional and easier to estimate accurately.
- `threshold = None`: no coefficient thresholding is applied, preserving the plug-in estimator form and simplifying theoretical analysis.

---

**Algorithm 2:** Smooth conditional Wasserstein distance

---

**Input:** i.i.d. sample  $((Y_i(0), Z_i(0)), 1 \leq i \leq n)$  drawn from  $P$ , i.i.d. sample  $((Y_j(1), Z_j(1)), 1 \leq j \leq m)$  drawn from  $Q$

**Output:**  $\widehat{CW}(\widehat{P}_n^\dagger, \widehat{Q}_n^\dagger)$

**Step 1:**

Compute the wavelet estimator  $\widehat{P}$  based on  $((Y_i(0), Z_i(0)), 1 \leq i \leq n)$  using Algorithm 1.

Compute the wavelet estimator  $\widehat{Q}$  based on  $((Y_j(1), Z_j(1)), 1 \leq j \leq m)$  using Algorithm 1.

**Step 2:**

Compute the wavelet estimator of  $\widehat{R} = (\widehat{P}_Z + \widehat{Q}_Z)/2$ .

Denote  $\widehat{P}_n^\dagger = \widehat{P}_n^\dagger(dy, dz) = \widehat{P}_Y^z(dy)\widehat{R}(dz)$ .

Denote  $\widehat{Q}_n^\dagger = \widehat{Q}_n^\dagger(dy, dz) = \widehat{Q}_Y^z(dy)\widehat{R}(dz)$ .

**Step 3:**

Sample  $(\tilde{Z}_\tau, 1 \leq \tau \leq N_Z := \lfloor (n \vee m) \log(n \vee m) \rfloor)$  from  $\widehat{R}$ .

**Step 4:**

**for**  $\tau = 1$  **to**  $N_Z$  **do**

    Let  $z = \tilde{Z}_\tau$ ,  $N_Y = \lfloor (n \vee m)^{(d_Y/4) \vee 1} \log(n \vee m) \rfloor$ ;

    Sample  $(Y_k^\tau(0), 1 \leq k \leq N_Y)$  from  $\widehat{P}_Y^z$ ;

    Sample  $(Y_l^\tau(1), 1 \leq l \leq N_Y)$  from  $\widehat{Q}_Y^z$ ;

    Compute

$$\widehat{W}_2^2(\widehat{P}_{\tilde{Z}_\tau}, \widehat{Q}_{\tilde{Z}_\tau}) := W_2^2\left(\frac{1}{N_Y} \sum_{k=1}^{N_Y} \delta_{Y_k^\tau(0)}, \frac{1}{N_Y} \sum_{l=1}^{N_Y} \delta_{Y_l^\tau(1)}\right)$$

    using the Python Optimal Transport (POT<sup>3</sup>) library [11];

**end**

**Step 5:**

Define

$$\widehat{CW}(\widehat{P}_n^\dagger, \widehat{Q}_n^\dagger) := \frac{1}{N_Z} \sum_{\tau=1}^{N_Z} \widehat{W}_2^2(\widehat{P}_{\tilde{Z}_\tau}, \widehat{Q}_{\tilde{Z}_\tau}).$$

**return**  $\widehat{CW}(\widehat{P}_n^\dagger, \widehat{Q}_n^\dagger)$

---

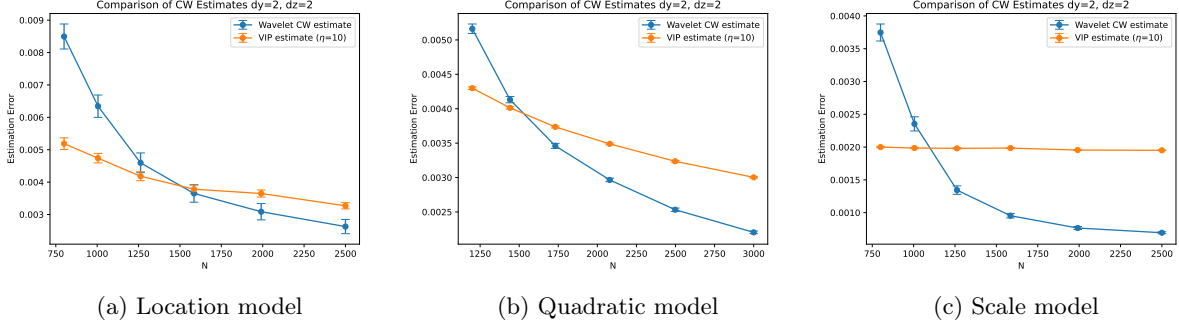


Figure 5: Plots of estimation error comparison of our method (*Wavelet CW estimate*) and [29] (*VIP estimate* with  $\eta = 10$ ) with  $d_Y = 2$ ,  $d_Z = 2$ . The estimation error is defined by  $\mathbb{E}[|V_c - \widehat{V}_c|]$ . The mean error curve and the corresponding 90% standard-error confidence bands are computed by aggregating results over 300 Monte Carlo repetitions.

- **nonnegativity = True**: enforces nonnegativity of the reconstructed density, preventing oscillations from producing negative values.
- **renormalize = True**: rescales the estimated density to integrate to one, ensuring it is a valid probability density.
- (i)  $N_z = 200$ ,  $N_y = 300$  (**location model**), (ii)  $N_z = 50$ ,  $N_y = 300$  (**quadratic model**), (iii)  $N_z = 100$ ,  $N_y = 600$  (**scale model**): number of grid points used to discretize the supports of  $Z$  and  $Y$  when numerically evaluating the conditional Wasserstein functional.

### E.1.2 Additional Estimation Result

In Figure 5, we show the plots of convergence rate corresponding to Figure 2.

## E.2 Simulation Details of Inference

### E.2.1 Data Generation Mechanism

In all scenarios,

$$Y(w) \mid Z = z \sim \mathcal{N}(\mu_w(z), \Sigma_w), \quad w \in \{0, 1\}.$$

**Scenario 1:**  $d_Y = 2$ ,  $d_Z = 1$

$$\begin{aligned} \mu_0(z) &= \begin{pmatrix} 0.35 \\ 0.55 \end{pmatrix} + \begin{pmatrix} 0.10 \\ -0.05 \end{pmatrix} z, \\ \mu_1(z) &= \mu_0(z) + \begin{pmatrix} 0.12 \\ -0.08 \end{pmatrix} + \begin{pmatrix} 0.10 \\ 0.02 \end{pmatrix} z, \\ \Sigma_0 &= \begin{pmatrix} 0.05^2 & 0 \\ 0 & 0.03^2 \end{pmatrix}, \quad \Sigma_1 = \begin{pmatrix} 0.07^2 & 0.01 \cdot 0.07 \cdot 0.04 \\ 0.01 \cdot 0.07 \cdot 0.04 & 0.04^2 \end{pmatrix}. \end{aligned}$$

**Scenario 2:**  $d_Y = 2$ ,  $d_Z = 2$  (**default**)

$$\begin{aligned} \mu_0(z) &= \begin{pmatrix} 0.35 \\ 0.55 \end{pmatrix} + \begin{pmatrix} 0.20 & -0.10 \\ 0.05 & 0.15 \end{pmatrix} z, \\ \mu_1(z) &= \mu_0(z) + \begin{pmatrix} 0.12 \\ -0.08 \end{pmatrix} + \begin{pmatrix} 0.10 & 0.04 \\ 0.02 & 0.06 \end{pmatrix} z. \end{aligned}$$

$$\Sigma_0 = \begin{pmatrix} 0.05^2 & 0 \\ 0 & 0.03^2 \end{pmatrix}, \quad \Sigma_1 = \begin{pmatrix} 0.07^2 & 0.01 \cdot 0.07 \cdot 0.04 \\ 0.01 \cdot 0.07 \cdot 0.04 & 0.04^2 \end{pmatrix}.$$

**Scenario 3:**  $d_Y = 3$ ,  $d_Z = 2$

$$\mu_0(z) = \begin{pmatrix} 0.35 \\ 0.55 \\ 0.45 \end{pmatrix} + \begin{pmatrix} 0.20 & -0.10 \\ 0.05 & 0.15 \\ -0.12 & 0.08 \end{pmatrix} z,$$

$$\mu_1(z) = \mu_0(z) + \begin{pmatrix} 0.12 \\ -0.08 \\ 0.05 \end{pmatrix} + \begin{pmatrix} 0.10 & 0.04 \\ 0.02 & 0.06 \\ -0.03 & 0.01 \end{pmatrix} z.$$

$$\Sigma_0 = \begin{pmatrix} 0.05^2 & 0 & 0 \\ 0 & 0.03^2 & 0 \\ 0 & 0 & 0.04^2 \end{pmatrix}, \quad \Sigma_1 = \begin{pmatrix} 0.07^2 & 0.01 \cdot 0.07 \cdot 0.04 & 0 \\ 0.01 \cdot 0.07 \cdot 0.04 & 0.04^2 & 0 \\ 0 & 0 & 0.05^2 \end{pmatrix}.$$

### E.2.2 Wavelet Algorithm Parameters

- **wavelet = "db4"**: Daubechies-4 wavelet basis, chosen for compact support and good smoothness properties.
- **mode = "periodization"**: boundary handling rule that treats the support as periodic, avoiding boundary artifacts for data supported on  $[0, 1]^d$ .
- **J\_joint = 4**: wavelet resolution level for estimating the joint density  $\hat{p}_{Y,Z}(y, z)$ . Larger values lead to finer resolution (lower bias, higher variance) and constitute the primary smoothing parameter.
- **J\_z = 6**: wavelet resolution level for estimating the marginal density  $\hat{p}_Z(z)$ . A higher level is used since  $Z$  is lower dimensional and easier to estimate accurately.
- **threshold = None**: no coefficient thresholding is applied, preserving the plug-in estimator form and simplifying theoretical analysis.
- **nonnegativity = True**: enforces nonnegativity of the reconstructed density, preventing oscillations from producing negative values.
- **renormalize = True**: rescales the estimated density to integrate to one, ensuring it is a valid probability density.
- $N_z = 120$ ,  $N_y = 120$ : number of grid points used to discretize the supports of  $Z$  and  $Y$  when numerically evaluating the conditional Wasserstein functional.

### E.3 Inference

In Figure 6, we illustrate the asymptotic distribution of our estimator  $CW_2^2(\hat{P}_n^\dagger, \hat{Q}_n^\dagger)$  for  $d_Y = 2$ ,  $d_Z = 1$ . In Figure 7, we present the corresponding asymptotic distribution for  $d_Y = 3$ ,  $d_Z = 2$ . The results are consistent with those in Section 4.2: larger sample sizes decrease the bias and improve the normality.

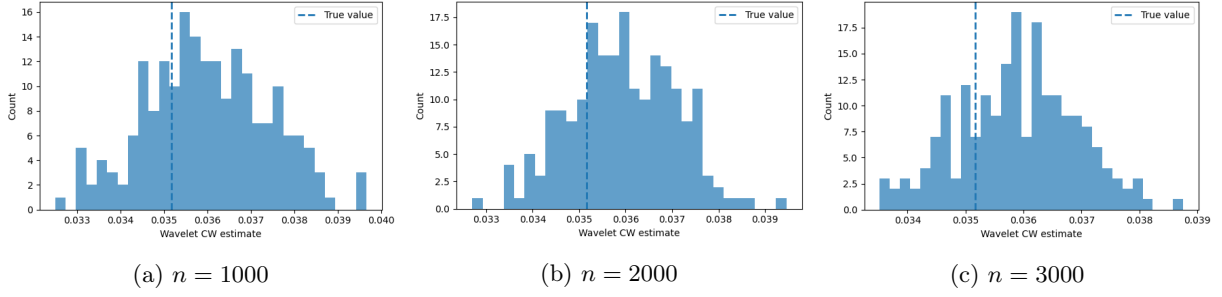


Figure 6: Histogram of the proposed estimator with the true value marked by a vertical dashed line. Here the default setting  $d_Y = 2$ ,  $d_Z = 1$  is adopted. The results are aggregated over 200 Monte Carlo repetitions.

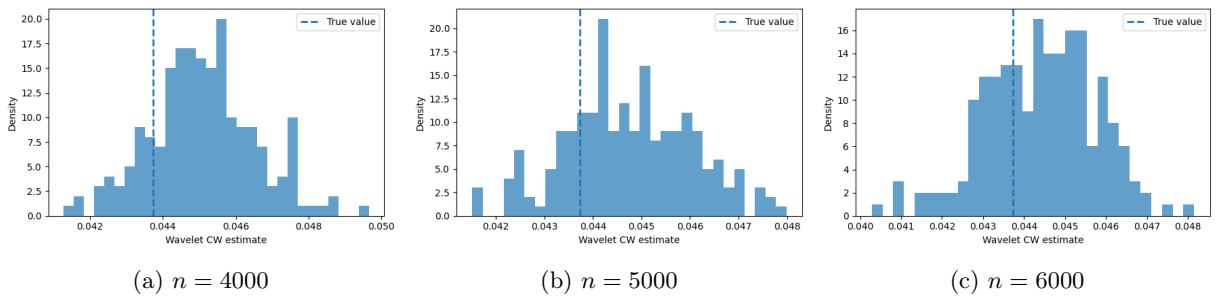


Figure 7: Histogram of the proposed estimator with the true value marked by a vertical dashed line. Here the default setting  $d_Y = 3$ ,  $d_Z = 2$  is adopted. The results are aggregated over 200 Monte Carlo repetitions.